


RESEARCH

Open Access



# Protection of lipopolysaccharide-induced otic injury by a single dose administration of a novel dexamethasone formulation

Silvia Murillo-Cuesta<sup>1,2,3\*</sup> , Ester Lara<sup>1,2</sup>, Jose M. Bermúdez-Muñoz<sup>1,2,3</sup>, Elena Torres-Campos<sup>1,2</sup>, Lourdes Rodríguez-de la Rosa<sup>1,2,3</sup>, Pilar López-Larrubia<sup>1,3</sup>, Signe R. Erickson<sup>4</sup> and Isabel Varela-Nieto<sup>1,2,3\*</sup>

## Abstract

**Background** The blood-labyrinth barrier (BLB) separates the inner ear from the circulation and is critical for maintaining ionic homeostasis and limiting the entry of deleterious agents. BLB integrity is disrupted by bacterial lipopolysaccharide (LPS), which elicits a strong inflammatory response in the inner ear leading to irreversible otic damage. Prolonged administration of systemic corticosteroids is the available treatment, but it shows both limited efficacy and major adverse effects. SPT-2101 is a novel in situ-forming gel formulation of dexamethasone allowing slow and sustained drug release after single intratympanic administration.

**Methods** We used a rat model of LPS-induced injury to define the functional, cellular and molecular mechanisms associated to BLB dysfunction and the protection by SPT-2101. Hearing was assessed by auditory brainstem response (ABR) recording, BLB permeability by gadolinium dynamic contrast-enhanced magnetic resonance imaging (DCE-MRI) and Evans blue extravasation. Gross cochlear histology and cellular alterations were studied by hematoxylin-eosin staining and immunofluorescence. RT-qPCR, PCR array and western blotting were used to assess transcriptional and protein changes.

**Results** LPS-challenged rats showed BLB breakdown and altered permeability as shown by the progressive increase in cochlear gadolinium uptake and Evans blue incorporation. LPS administration increased the cochlear expression of the LPS toll-like receptors *Tlr2* and co-receptor *Cd14*, pro-inflammatory cytokines and receptors such as *Il1b* and *Il1r1*, and also the oxidative stress and inflammasome mediators NRF2 and NLRP3. LPS also increased IBA1-positive macrophage infiltration in the lateral wall and spiral ganglion. A single intratympanic injection of SPT-2101 protected BLB integrity and prevented otic injury. Comparable effects were obtained by repeated administration of systemic dexamethasone, but not by a single dose. SPT-2101 administration normalized molecular inflammatory mediators and suppressed macrophage infiltration.

\*Correspondence:

Silvia Murillo-Cuesta  
smurillo@iib.uam.es  
Isabel Varela-Nieto  
ivarela@iib.uam.es

Full list of author information is available at the end of the article



© The Author(s) 2023. **Open Access** This article is licensed under a Creative Commons Attribution 4.0 International License, which permits use, sharing, adaptation, distribution and reproduction in any medium or format, as long as you give appropriate credit to the original author(s) and the source, provide a link to the Creative Commons licence, and indicate if changes were made. The images or other third party material in this article are included in the article's Creative Commons licence, unless indicated otherwise in a credit line to the material. If material is not included in the article's Creative Commons licence and your intended use is not permitted by statutory regulation or exceeds the permitted use, you will need to obtain permission directly from the copyright holder. To view a copy of this licence, visit <http://creativecommons.org/licenses/by/4.0/>.

**Conclusions** Our data indicate that single local administration of dexamethasone formulated as SPT-2101 protects BLB functional integrity during endotoxemia, providing a novel therapeutic opportunity to treat diseases related to BLB dysfunction.

**Keywords** Corticosteroids, Bacterial infection, DEX-nanoformulation, Inflammation, Innate immune response, MRI, TLR, Strial vascular permeability

## Background

The blood-labyrinth barrier (BLB) in the stria vascularis is a highly specialized capillary network of endothelial cells linked by tight junctions and the basement membrane, and in close contact with surrounding pericytes and perivascular macrophage-like melanocytes [1]. Akin to the blood-brain barrier, the BLB functions as a selective barrier, allowing the passage of nutrients, ions and fluids into the cochlea, and restricting the entry of antigens, toxic substances and immune cells. It thus has a critical role in maintaining cochlear homeostasis and defense, and BLB alteration has been associated with a wide range of pathological conditions [2].

The cochlea was traditionally considered as an immune-isolated organ due to the existence of this BLB. However, numerous studies confirm that it possesses a well-established immune cell population capable of triggering local inflammatory responses and interacting with the systemic immune system to protect against infection and cell injury [3, 4]. Bone marrow-derived resident macrophages represent the main elements of the cochlear immune system and have been identified in the spiral ligament, spiral limbus, stria vascularis, basilar membrane, modiolus, and the osseous spiral lamina [4]. In addition to macrophages, other cells are involved in immune and inflammatory response in the inner ear. For instance, hair cells and supporting cells in the organ of Corti express immune-related genes, including toll-like receptors (TLRs), signal transducers, and chemokines [5, 6]. Perivascular macrophage-like melanocytes also function both in immune response and in maintaining BLB integrity [7, 8]. Furthermore, circulating immune cells, monocytes, and neutrophils, are recruited to the cochlea in response to noxious stimuli, and contribute to inflammatory responses [9].

The cochlear immune system is activated in response to infections, acoustic trauma, ototoxic drugs, age-related cochlear degeneration, and surgery [4]. Bacterial infections are frequently caused by Gram-negative bacteria, whose outer membrane contains lipopolysaccharide (LPS or endotoxin), a potent activator of the immune system [10], and can be modeled in animals by administering LPS, either systemically or locally [10, 11]. LPS exerts its effects through binding to toll-like receptor 4 (TLR4) on immune cells, particularly in resident macrophages in the spiral ligament, and activating downstream MyD88- and TRIF-signaling pathways. This event ultimately leads

to triggering of transcription factors such as NF $\kappa$ B or IRF3 and the production and secretion of several cytokines, chemokines and vasoactive substances, including IL-1B, IL-6, IL-8, NF $\kappa$ B, TNFA, PGE2, ROS, nitric oxide, ICAM, and interferons [12]. Mild tissue damage can occur as the result of inflammatory mediators release by activated macrophages, but in the absence of a real bacterial infection, this immune activity quickly resolves. However, chronic infections or the presence of a second insult (antibiotics, cisplatin or noise) can induce a strong and occasionally exacerbated immune reaction, leading to further cochlear damage and loss of hearing [13].

Beyond activating cochlear inflammatory responses, LPS can cause BLB disruption, which alters cochlear vascular permeability and triggers stria swelling [14]. Indeed, cytokines released after LPS exposure impair the tight junctions between endothelial cells and induce the detachment of pericytes and perivascular macrophages from the capillary wall, which reduces their contacts with endothelial cells, ultimately compromising the BLB integrity [15, 16]. These structural changes are associated with an increase in the expression of matrix metalloproteinases and with a decrease in the expression of tight junction proteins [16–18].

LPS-induced loss of BLB integrity and altered permeability have damaging effects in the inner ear in terms of potassium recycling and endolymph homeostasis, potentially leading to hearing loss [11, 19, 20]. In addition, disrupted BLB allows the entry of blood-borne antigens or toxic substances. Indeed, an exacerbation of ototoxicity of aminoglycosides or cisplatin is observed during LPS inflammation [14, 21, 22]. For this reason, the assessment of BLB integrity and function is receiving increased attention in Otorhinolaryngology clinics [2]. Magnetic resonance imaging (MRI) using gadolinium-based contrast agents is a useful tool to assess BLB integrity, both in animal models and in the clinical practice [23, 24]. Gadolinium crosses the BLB in healthy ears, enhancing the visualization of the perilymphatic space on MRI. Changes in BLB integrity increase the permeability to gadolinium, which enhances MRI signal.

BLB disruption secondary to cochlear immune and inflammatory responses is a potential contributor to the pathogenesis of hearing loss, and have been associated not only with middle and inner ear infections, but also with autoimmune disorders, acoustic trauma, ototoxicity, presbycusis, and Meniere's disease, among others

[11, 25–28]. Preventing inner ear inflammation is thus a clinical aspiration [29]. The most widely used strategy for reducing inflammation is administration of corticosteroids, mostly dexamethasone [30]. Corticosteroids exert their immunosuppressive effects by binding to cytoplasmic glucocorticoid receptors, which have been identified in the cochlea [31].

Systemic administration of steroid drugs is the preferred route in everyday clinical practice, but high doses are needed to reach therapeutic concentrations across the BLB, which can lead to systemic side effects [30]. Injection through the tympanic membrane into the middle ear is an alternative modality that bypasses the BLB and minimizes systemic effects [32]. However, steroid solutions clear quickly from the middle ear and, therefore, require frequent administration. Consequently, there is interest in the development of novel delivery systems that achieve sustained drug delivery into the inner ear with a single administration. In this context, SPT-2101 is a cross-linking gel formulation of dexamethasone with bioadhesive and shape-conforming properties that is designed for sustained release in the middle ear. SPT-2101 is currently being tested in a phase 1 clinical trial for the treatment of Meniere's disease BLB alterations (ACTRN12621000964819).

Here we evaluated the therapeutic efficacy of a single intratympanic administration of SPT-2101 to attenuate the functional, molecular, and cellular cochlear processes triggered by LPS, using an *in vivo* model of endotoxemia-induced inflammation.

## Methods

### Experimental animals and treatments

Male and female albino Wistar rats (RjHan:WI, 5–6 weeks of age, 150–225 g; Janvier Labs) were used. No differences were observed between sexes and data were aggregated. Rats were randomly allocated into the following experimental groups: control, LPS only, LPS plus vehicle, and LPS plus SPT-2101. LPS (*Escherichia coli* O55:B5, #L2880, Sigma-Aldrich) was prepared in saline, and rats received intraperitoneal (i.p.) injections of 5 mg/kg and 10 mg/kg over 2 consecutive days (Fig. 1A). LPS induced inactivity, dyspnea and diarrhea after the first injection, and resulted in 20% mortality at 24 h. SPT-2101 was prepared as a suspension of 6% (w/w) dexamethasone in a vehicle comprising 0.2% (w/w) trilycine acetate and 8.3% (w/w) pentaerythritol poly(ethylene glycol). Drug and vehicle components were provided by Spiral Therapeutics (San Francisco). SPT-2101 or vehicle (30  $\mu$ L) was administered by unilateral intratympanic injection [33] 3 days before LPS challenge. To compare the efficacy of local *versus* systemic routes, an additional group of rats received dexamethasone (Kern Pharma; 4 mg/mL EFG injectable solution) i.p. (5 mg/kg), for

1 day or for 3 consecutive days, beginning 1 or 3 days before LPS administration, respectively.

### In vivo functional studies

Hearing was evaluated by registering the auditory brainstem response (ABR) to sound stimuli with an Auditory Workstation (Tucker Davis Technologies) running BioSigRZ software, as described [34]. Briefly, click and tone burst (8–40 kHz) stimuli were delivered at decreasing intensities from 90 to 10 dB SPL in steps of 5 or 10 dB. Electroencephalographic responses were registered with subdermal electrodes (TE/S50716-001; Technomed) located at the vertex (register), mastoid (reference), and back (ground) regions, amplified and averaged. ABR thresholds were defined as the minimum sound level that elicited a clearly identifiable ABR wave pattern with mean peak amplitude above 200 nV in response to click and tone stimuli.

Cochlear vascular permeability was evaluated by dynamic contrast-enhanced magnetic resonance imaging (DCE-MRI). Images were acquired on a horizontal 7.0-Tesla Bruker BioSpec<sup>®</sup> system (Bruker Medical GmbH) with a 40-mm inner diameter radiofrequency coil and a maximum gradient strength of 360 mT/m, running ParaVision 6.0.1 on a Linux environment. Rats were scanned at different time points (0.5, 1, 2, 4, 25, 48 and 72 h) after the first LPS injection (Fig. 1A).  $T_1$ - and  $T_2$ -weighted images ( $T_1W$  and  $T_2W$ ) were acquired to identify the regions of interest (ROIs), which were followed with a DCE-MRI routine involving the acquisition of a series of images before, during, and after administration of a contrast agent [24]. Specifically, a set of 45 cycles (0.8 min/cycle) of  $T_1W$  MR images were acquired with the following parameters: TR/TE=200/10 ms, 8 slices of 1.5-mm thickness, with no-gap, in horizontal (axial) orientation, with a spatial resolution of  $0.148 \times 0.148$  mm<sup>2</sup>, and a total acquisition time of 36 min. A single 0.3 mmol/kg intravenous bolus of gadobutrol, a gadolinium-based contrast agent (Gadovist; Bayer) was administered 5 min after the initiation of the acquisition (corresponding to ~7th cycle). Data analysis was performed with the Fiji “multi-measure” plugin to follow-up gadobutrol distribution in the inner ear and surrounding tissues. Normalized values were calculated by comparison with an external reference. The signal enhancement in the cochlear ROIs was defined as the ratio of the signal intensity in a specific MRI cycle with respect to the signal intensity obtained in the first cycle, and reflects time-dependent modifications in the tissue signal intensity due to the different concentration of gadobutrol in the tissues.

BLB permeability was also assessed with Evans blue uptake [18]. A 2% solution of the tracer (#E2129; Sigma-Aldrich) in saline was prepared and injected (2 mL/kg)

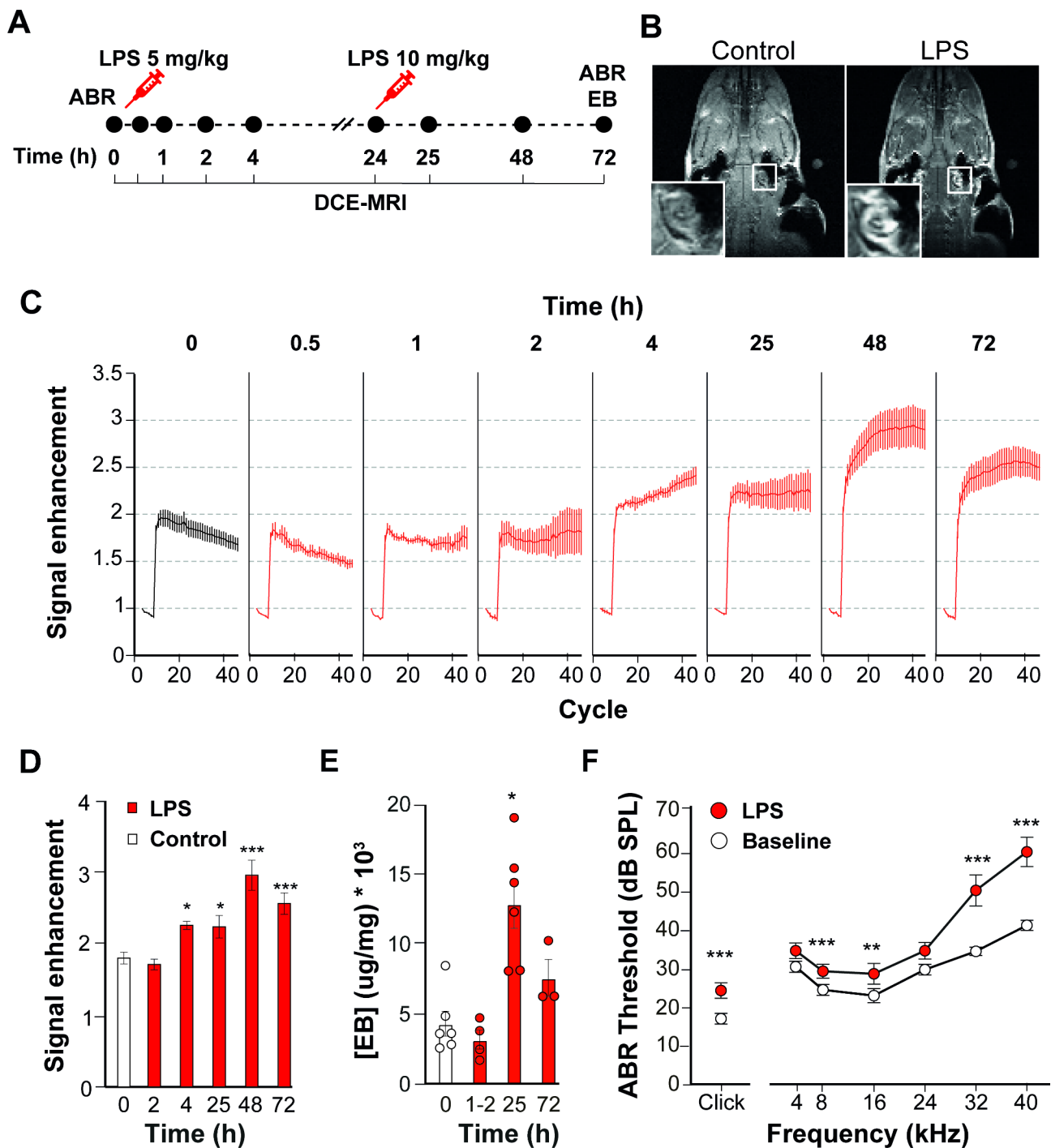


**Fig. 1** LPS challenge increases BLB permeability and causes hearing loss. **(A)** Experimental design scheme. LPS was injected IP at 5 and 10 mg/kg on two consecutive days. Dynamic contrast-enhanced magnetic resonance imaging (DCE-MRI; 45 cycles, IV injection of contrast agent at cycle 7), Evans blue (EB) level quantification and auditory brainstem responses (ABR) recording were performed at different time points after LPS challenge. **(B)** Representative T1-weighted horizontal head images obtained at the end of DCE-MRI in rats from control and LPS groups, 72 h after challenge. Detail of the cochlea is shown in the white square. **C-D)** Time-course of the signal enhancement (mean  $\pm$  SE) along the DCE-MRI **(C)** or in a representative 30th cycle **(D)** in control rats without LPS (white;  $n=16$  for time 0 h) and in LPS-injected rats (red;  $n=4$  rats for 0.5, 1, 2 and 4 h;  $n=8-9$  for 25 and 48 h and  $n=16$  for 72 h). **E)** EB concentration (mean  $\pm$  SE, in  $\mu\text{g}/\text{mg}$ ) in the inner ear from control (white,  $n=6$ ) and LPS-injected rats (red,  $n=3-6$ ), 1-2, 25 and 72 h after LPS challenge. **F)** ABR thresholds (mean  $\pm$  SE, in dB SPL) before (white circles) and 72 h after (red circles) LPS injection in rats from the LPS group ( $n=31$ ). Statistically significant differences were calculated using Kruskal-Wallis **(D, E)** or Mann-Whitney **(F)** tests (\* $p < 0.05$ , \*\* $p < 0.01$ , \*\*\* $p < 0.001$ )

into the tail vein of isoflurane-anesthetized rats 1–2, 25 or 72 h after the first LPS injection.

One hour after tracer injection, rats were sacrificed by pentobarbital overdose (Dolethal, Vetoquinol, 150 mg/kg) and perfused with 300 mL PBS to remove the tracer from the circulatory system, and cochleae were dissected and stored at  $-80^{\circ}\text{C}$  for analysis. Trichloroacetic acid (1:1 volume in saline) was added to the sample (3:1), which was then homogenized in a TissueLyser LT (Qiagen) at 50 Hz for 6 min. The supernatant was separated by centrifugation ( $103 \times g$  for 20 min), collected and diluted 1:3 by volume in 95% ethanol. Fluorescence was measured in a Glomax™ Luminometer and Microplate Reader (Promega) (620/680 nm excitation/emission wavelength).

### Cochlear histology and immunofluorescence

Rats were sacrificed by pentobarbital overdose 72 h after the first LPS injection, and were intracardially perfused with 0.1 M PBS followed by 4% paraformaldehyde (PFA; Merck) in 0.1 M PBS. Dissected inner ears were post-fixed with 4% PFA, decalcified in 5% EDTA (Sigma-Aldrich) and embedded in paraffin or Tissue-Tek® OCT (Sakura Finetek). Whole mount dissections of the organ of Corti or stria vascularis were used in some analyses.

Paraffin Sect. (5  $\mu\text{m}$ ) parallel to the modiolus were prepared on an RM2155 microtome (Leica Microsystems) and stained with hematoxylin-eosin. Images were acquired using a Zeiss AxioPhot microscope (Carl Zeiss). Gross cochlear cytoarchitecture and stria vascularis morphology was evaluated in mid-modiolar paraffin sections. The stria vascularis area was calculated with the Fiji “segmented line” tool.

Frozen Tissue-Tek® Sect. (10  $\mu\text{m}$ ) were obtained on a Cryocut 1950 (Leica Microsystems) and used for immunodetection (ab5076; goat anti-IBA1 1:100; Abcam). Sections were mounted with Vectashield Mounting Medium containing DAPI (Vector Laboratories) and images were acquired on epifluorescence (Nikon 90i) and confocal laser-scanning (Zeiss LSM710) microscopes. IBA1 was quantified for each cochlear turn in serial cryosections using Fiji software as described [34, 35].

Stria vascularis whole mounts were prepared as described [16]. They were first incubated overnight at  $4^{\circ}\text{C}$  with lectin *Griffonia simplicifolia* IB4 (GS-IB4) conjugated to Alexa Fluor 568 (1:50, I21412, Life Technologies) and with rabbit anti-Desmin (1:50, AB32362; Abcam), and then incubated with the corresponding Alexa Fluor secondary antibody (1:100, A22287; Thermo Fisher Scientific) and DAPI (1:1000; Thermo Fisher Scientific) for 2 h at room temperature. Finally, stained samples were mounted using Fluoromount-G mounting medium (Southern Biotech). Stack images were acquired with a Zeiss LSM710 confocal laser-scanning microscope (40 $\times$ ). Desmin coverage of capillaries, shown as

percentage, was calculated as the ratio between the overlapped desmin/GS-IB4 area and the total GS-IB4 area (adapted from [16]).

Organ of Corti whole mounts preparation and hair cell and synapse quantification were performed as reported [34, 35]. Decalcified cochleae were divided into 5 half-turns from apex to base and labeled with rabbit anti-Myo7a (1:150, PT-25-6790; Proteus), mouse anti-CtBP2 (1:200, 612,044; BD Biosciences) and mouse anti-GluR2/3 (1:1000, MAB397; Millipore) antibodies. Sections were incubated with corresponding Alexa Fluor secondary Goat Alexa Pacific Blue anti-rabbit (1:200, P10994; Invitrogen), Goat Alexa 488 anti-mouse-IgG1 (1:500, A-21,121) and Goat Alexa 555 anti-mouse-IgG2a (1:500, A-21,137; Thermo Fisher) antibodies for 1 h at  $37^{\circ}\text{C}$ . The half-turns were then stained with TO-PRO3 (1:750, T-3605; Invitrogen) and mounted with Prolong Diamond reagent (Thermo Fisher). Low magnification fluorescent images were captured on a Nikon 90i fluorescence microscope and used for cochleogram analysis using a custom Fiji plugin [36]. Representative fluorescent tile scan and z-stack images were acquired with a Zeiss LSM710 confocal laser-scanning microscope. The number of inner (IHC) and outer (OHC) hair cells were counted in 200  $\mu\text{m}$  of the basilar membrane in the 4 (apical), 16 (middle), and 32–40 (basal) kHz regions located 15–20%, 30–35%, and 80–90%, respectively, of the total distance from the apex. Co-localized presynaptic ribbons and postsynaptic glutamate receptor patches were counted from each confocal z-stack using IMARIS (Bitplane Inc.). A spot of each signal (CtBP2 and GluR2/3) was created in independent channels using an XY diameter of 0.8  $\mu\text{m}$  for CtBP2 and GluR2/3, a corrected PSF Z-diameter of 1.5  $\mu\text{m}$ , and using a background subtraction function. Spot co-localization was used to determine pairing of presynaptic and postsynaptic elements. A threshold of 1  $\mu\text{m}$  was set to define the juxtaposition of two different puncta.

### Gene expression and western blotting

Inner ears were dissected and cochleae were separated from vestibules and immediately immersed in RNAlater® (Sigma-Aldrich). RNA extraction, quality determination and cDNA synthesis were performed as reported [34, 37]. Quantitative analysis of individual cochlear extracts was performed in triplicate on a QuantStudio™ 7 Flex Real-Time PCR System (Applied Biosystems) using TaqMan probes (*Foxp3* [Rn01525092\_m1], *Il10* [Rn01483988\_g1], *Tbp* [Rn01455646\_m1]), or gene-specific primers (Supplementary Table S1). QuantStudio™ Real-Time PCR software 1.3 (Applied Biosystems) was used for data analysis. *Tbp* was the housekeeping gene and differential expression (RQ) between groups was calculated by the  $2^{-\Delta\Delta\text{Ct}}$  method using control rats as the calibrator

sample. The PCR array RT<sup>2</sup> Profiler™ Rat Innate & Adaptive Immune Responses (Qiagen, #PARN-052Z) was used with pooled cochlear RNA extracts (n=3) to generate cDNA, and quantitative amplification was performed in duplicate with the RT<sup>2</sup> SYBR® Green qPCR Mastermix (Qiagen, #330,529). Data were analyzed using Geneglobe (Qiagen), with a Ct cut-off set to 35. The mean of *Hprt1* and *Rplp1* Cts was used as the normalization factor based on an automatic selection from a housekeeping panel of reference genes. Heatmapper was used to generate the heatmap from average mean  $2^{-\Delta Ct}$  values for each condition and time-point [38].

Whole cochlea protein extracts (from one cochlea) were homogenized in ice-cold RIPA buffer supplemented with 0.01% phosphatase (#P5726) and protease inhibitors (#P8340) (Sigma-Aldrich) using a bead homogenizer (TissueLyser LT). Extracts were centrifuged at  $14,000 \times g$  for 10 min at 4 °C and supernatants were used for western blotting. Equal amounts of protein (quantified by Bradford Assay; Bio-Rad Laboratories) were resolved by SDS-PAGE (8%) electrophoresis, followed by transfer to PVDF membranes using a Bio-Rad Trans Blot TURBO (Bio-Rad Laboratories). After incubation with 5% bovine serum albumin or non-fat dried milk in 0.1% Tween/1 mM TBS, membranes were probed overnight at 4 °C with the primary antibodies and then with the corresponding peroxidase-conjugated secondary antibody for 1 h at room temperature. Primary antibodies used were as follows: rabbit anti-NLRP3 (D4D8T) (1:1000; 15,101; Cell Signaling Technology), rabbit anti-NRF2 (1:1000; *in house*), and mouse anti-vinculin (1:20000; sc-73,614; Santa Cruz Biotechnology). Immunoreactive bands were revealed using the Clarity™ Western ECL Substrate (Bio-Rad), and images were captured with the ImageQuant LAS4000 mini digital camera using ImageQuant TL software 8.1 (GE Healthcare).

### Statistical analysis

Data for ABR, MRI, Evans blue and LPS time-course RT-qPCR were analyzed and plotted with SPSS v27 software (IBM). General histology and immunofluorescence, PCR array and RT-qPCR (except LPS time-course) data were analyzed and plotted with Graphpad Prism (GraphPad Software). Data are expressed as mean  $\pm$  SE. Statistical significance was analyzed by one-way ANOVA, Kruskal-Wallis or Mann-Whitney tests following Shapiro-Wilk and Brown-Forsythe tests to determine normality and homogeneity of variances, respectively (\*  $p < 0.05$ ; \*\*  $p < 0.01$ ; \*\*\*  $p < 0.001$ ).

## Results

### SPT-2101 treatment protects against greater cochlear permeability induced by lipopolysaccharide

First, we evaluated the LPS-induced changes on BLB permeability, hearing, cochlear morphology and inflammatory gene cochlear expression, and then the effect of SPT-2101 pretreatment in rats challenged with LPS.

LPS has a rapid effect on the BLB permeability (assessed by DCE-MRI), increasing gadobutrol uptake and therefore the MRI signal in the cochlea (Fig. 1B). Analysis of the T<sub>1</sub>W signal along the DCE-MRI acquisition in control animals (non-LPS-challenged, time 0 h) revealed an increase in signal intensity in the cochlea immediately after gadolinium injection (cycle 7; 5 min after starting the scan), which was followed by a progressive decrease over the course of 30 min (Fig. 1C). A time-course analysis of the DCE-MRI signal enhancement showed slight changes in the signal enhancement profile 1 h after LPS administration, which were potentiated after the second LPS dose (Fig. 1C). Statistical analysis of the MRI signal enhancement in a representative cycle (30th ) indicated a significant increase at 4 h ( $p < 0.05$ ), 25 h ( $p < 0.05$ ), 48 h ( $p < 0.001$ ) and 72 h ( $p < 0.001$ ) after LPS challenge over the baseline (time 0 h after LPS) (Fig. 1D). We confirmed the LPS-induced changes in cochlear permeability using Evans blue. Quantification of its levels after LPS challenge revealed a robust and significant ( $p < 0.05$ ) 3-fold increase 1 h following the second LPS injection (Fig. 1E).

LPS induced an increase in the ABR thresholds over baseline values, with significant differences for the click and also for 8,16, 32 and 40 kHz (Fig. 1F). General morphological evaluation of main cochlear structures indicated no evident alterations in the organ of Corti or spiral ganglion in LPS-challenged rats, compared to controls (Fig. 2A). Besides, quantification of cochlear hair cells and synaptic markers *Ctbp2* and *GluR2/3* in whole-mount preparations of the organ of Corti, confirmed that LPS did not cause obvious neurosensory cell or synapse loss (Fig. 2B-D). Therefore, the altered stria permeability induced by LPS suffices to cause hearing impairment.

A cochlear gene expression time-course study done in parallel indicated significant LPS-induced increases in the expression of toll-like receptors *Tlr4* (and of TLR4 signaling pathway cofactor *Cd14*) and *Tlr2*. *Tlr2* and *Cd14* expression peaked 4 h after the first dose and peaked again at 25 h (1 h after the second dose) (Fig. 3), whereas *Tlr4* expression began to increase after the second LPS dose and peaked at 72 h. Although TLR2 is not the canonical LPS-recognizing receptor, it is required for LPS-induced TLR4 signaling in some tissues [39]. LPS similarly induced the gene expression of inflammatory cytokines, particularly *Il1b* and *Il1ri*, and inflammatory mediators including *Nfkb*, *Inos* and *Cse*, with an initial peak 1 h (*Il1b*) or 2 h (*Il1ri*, *Nfkb* and *Inos*) after the

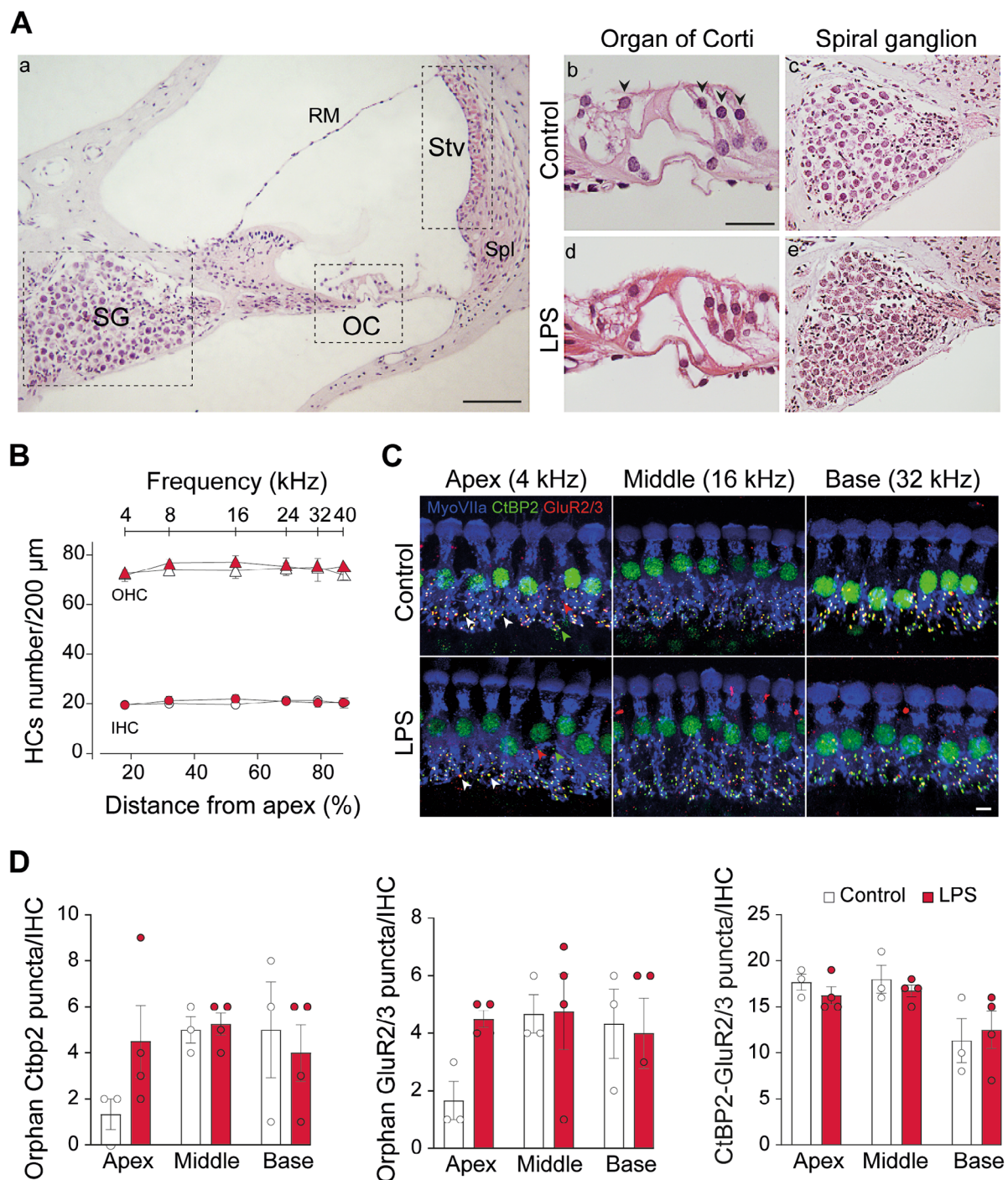


**Fig. 2** LPS challenge does not cause hair cell loss or synapse alterations. **(A)** Paraffin midmodiolar cochlear sections stained with hematoxylin-eosin. General view of the cochlear middle turn **(a)** and detail of the organ of Corti **(b, d)** and spiral ganglion **(c, e)** of rats from control and LPS experimental groups, 72 h after first injection, showing no evident alterations. Scale bar: 50  $\mu$ m **(a)** and 10  $\mu$ m **(b)**. **(B)** Inner (IHC) and outer (OHC) hair cell counts (mean  $\pm$  SE) in the organ of Corti from apical (4–8 kHz), middle (16–24 kHz) and basal (32–40 kHz) turns, in control (n=3, white) and LPS (n=4, red) rats, 72 h after challenge. **(C)** Representative confocal images of organ of Corti whole mounts at apical (4 kHz), middle (16 kHz) and basal (32–40 kHz) cochlear turns from control and LPS-injected rats, immunolabeled for MyoVIIa (blue), CtBP2 (green), and GluR2/3 (red) for synapse evaluation. Red and green arrowheads indicate individual post- and presynaptic marker staining, respectively, and white arrowheads indicate co-localized CtBP2-GluR2/3 puncta. Scale bar: 8  $\mu$ m. **(D)** Quantification of orphan CtBP2, orphan GluR2/3 and co-localized CtBP2-GluR2/3 puncta per IHC in control (n=3) and LPS-injected (n=4) rats. Data presented as mean  $\pm$  SE.

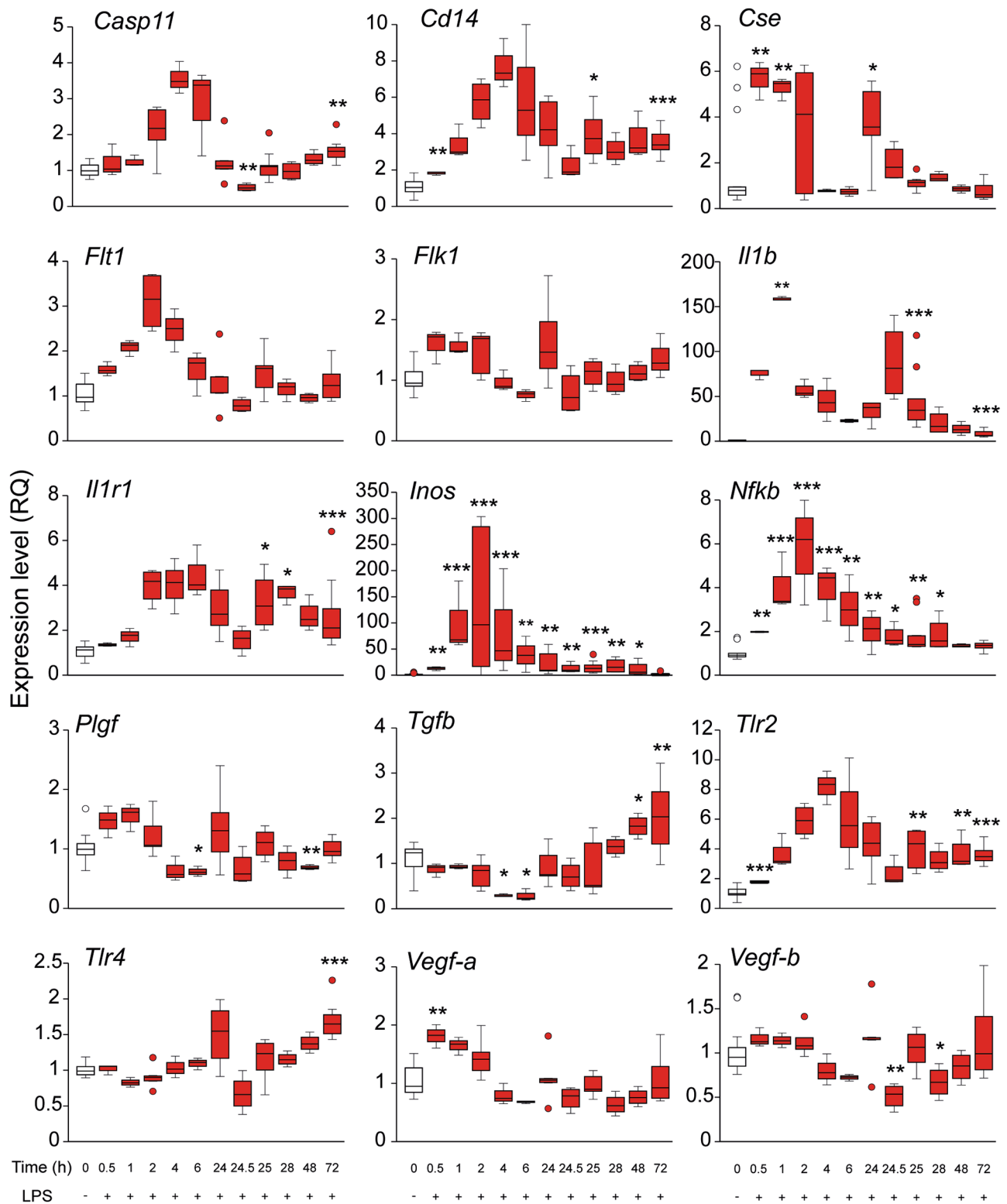


**Fig. 3** LPS challenge increases cochlear expression of LPS response machinery and inflammatory genes. Expression levels of genes related to inflammation and immune response, before and at different moments after LPS injection. Results were calculated as  $2^{-\Delta\Delta Ct}$  (RQ, expressed as mean  $\pm$  SEM), using *Tbp* as the reference gene and normalized to control rats without LPS (time 0 h). At least 3 rats were included for each timepoint (n = 15 rats for 0 h; n = 3–5 rats for 0.5, 1, 2, 4, 6, 24.5, 28 and 48 h; n = 9 for 25 h and n = 12 for 72 h). Statistically significant differences were calculated using one-way ANOVA or Kruskal-Wallis tests (\*p < 0.05; \*\*p < 0.01; \*\*\*p < 0.001)



first LPS dose and a second peak after the second dose (*Il1b* and *Il1r1*). The expression of all the aforementioned genes decreased to normal levels within 72 h. Contrastingly, the expression of *Tgfb* increased significantly 48 and 72 h after the first LPS injection. Finally, LPS also increased the expression of *Vegfa* (vascular endothelial growth factor), a key regulator of permeability, 30 min after LPS injection. No significant increases were observed in the expression of *Vegfb*, *Flk1*, *Flt1* and *Plgf* after LPS challenge.

We next explored changes in MRI, ABR, cochlear morphology and gene expression in LPS-injected rats pretreated with SPT-2101. SPT-2101 was administered by intratympanic injection 3 days before LPS challenge, and cochlear functional and molecular changes were evaluated 3 days after the first LPS injection (Fig. 4A).

Analysis of the  $T_1W$  signal intensity in the cochlea of control rats (non-SPT-2101 treated or LPS-challenged) revealed, as previously shown, a rapid increase immediately after gadolinium injection and a progressive decrease thereafter (Fig. 4B). LPS-challenged rats showed a similar initial increase in the  $T_1W$  signal intensity, but it raised further and remained elevated over the scanned period (Fig. 4B), which is consistent with increased gadolinium extravasation as a consequence of altered BLB permeability. On the contrary, rats administered SPT-2101 intratympanically 3 days before LPS challenge revealed no LPS-induced increase in the  $T_1W$  signal intensity, and the signal enhancement profile was comparable with that of control rats (Fig. 4B). This indicated that SPT-2101 pretreatment inhibits stria permeability changes and curbs gadolinium leakage. By contrast, the DCE-MRI profiles of LPS-challenged rats pretreated or not with vehicle were superimposable.

Analysis of the MRI signal enhancement in a representative cycle (30th ) of the experimental groups revealed significant differences between non-challenged and LPS-challenged rats, and a significantly reduced signal in rats pretreated with SPT-2101 before LPS challenge (Fig. 4C-D). Notably, the protective effect achieved by the single local administration of SPT-2101 was stronger than that observed with a single dose of systemic dexamethasone (5 mg/kg) and was similar to that achieved with repeated dexamethasone administration over 3 days (Fig. 4D). Finally, the LPS-induced ABR threshold shifts for 32 and 40 kHz sound stimuli were significantly lower in SPT-2101 pre-treated rats than in vehicle-treated rats (Fig. 4E).

#### **SPT-2101 treatment suppresses the morphological changes induced in the blood-labyrinth-barrier by lipopolysaccharide**

We next determined whether LPS changed the morphology of the stria vascularis and the cellular components of

the stria BLB, which would lead to impaired functional integrity. The stria vascularis in LPS-challenged rats was slightly enlarged, with statistically significant differences in the stria area in the middle cochlear turn compared to controls (30%;  $p < 0.05$ ), whereas rats pretreated with SPT-2101 before LPS challenge did not show this enlargement (Fig. 5A).

We further studied the BLB in stria vascularis whole-mount explants immunostained to visualize vascular capillaries (anti-GS-IB4) and pericytes (anti-Desmin). It has previously been shown that stria pericytes change their shape from flat and slender to round after LPS challenge, which reduces their physical contact with stria capillaries [16]. Stria whole-mounts analysis 72 h after LPS administration revealed vasodilatation of the capillaries and a rounded and branched morphology of pericytes, which separate from the blood vessels (Fig. 5B). We next assessed pericyte coverage of the stria capillaries by quantifying Desmin/GSIB4 co-localization. We found a significant increase in the coverage of the stria capillaries in LPS-challenged animals than in controls, whereas pre-treatment with SPT-2101 before LPS administration partially reversed this (Fig. 5C). We also studied stria integrity by examining the expression levels of tight-junction genes (*Tjp1*, *Cdh5* and *Marveld2*) and of pigment epithelium-derived factor (*Serpinf1*), which modulates tight junction protein expression in perivascular macrophages [25]. Compared with control rats, we found an increase in the expression of tight-junction genes in LPS-challenged rats, which was significant for *Cdh5* (1.5-fold;  $p < 0.01$ ). Analysis of *Serpinf1* expression in the three groups revealed that it was significantly lower (3-fold;  $p < 0.001$ ) in SPT-2101 pre-treated rats than in vehicle-treated rats before LPS challenge. Notably, *Cdh5* expression in SPT-2101 pre-treated rats was similar to control values (Fig. 5D).

#### **Lipopolysaccharide-induced changes in the expression of inflammatory genes are moderated by SPT-2101**

Systemic LPS challenge induced inflammatory responses in the cochlea, which included the activation of the innate immune system, recruitment of monocytes and macrophages, and the release of inflammatory cytokines. To explore the molecular mechanisms linking LPS-induced cochlear inflammation and changes in BLB permeability, we performed gene expression analysis of 84 innate and adaptive immune response genes in control and LPS-challenged rats at 4, 25 and 72 h following the first LPS dose, using a PCR array. Results showed that LPS induced the expression of gene clusters in a defined temporal manner (Fig. 6A). In control rats (with no LPS administration), 5 of the transcripts studied showed positive z-score values (*Rag1*, *Il2*, *Il4*, *Il5* and *Cd11d1*). Four hours following the LPS challenge, the transcription of

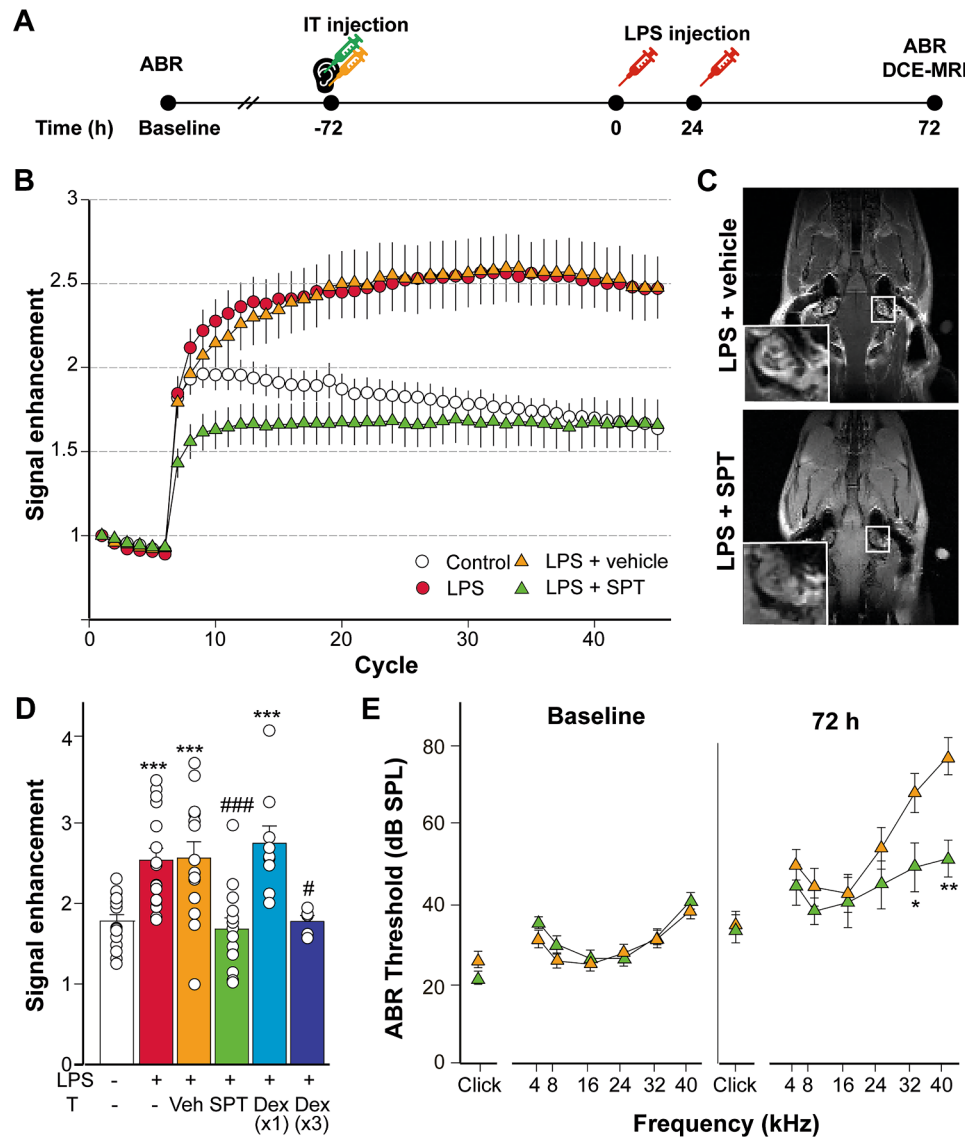


**Fig. 4** SPT-2101 prevents LPS-induced cochlear injury and hearing loss. **(A)** Experimental design scheme: LPS was injected IP at 5 and 10 mg/kg on two consecutive days. SPT-2101 (SPT) or its vehicle were intratympanically injected 72 h before LPS. Auditory brainstem responses (ABR) were recorded at the before (baseline) and 72 h after the first LPS challenge. At this endpoint, a dynamic-contrast enhanced magnetic resonance imaging (DCE-MRI; 45 cycles, IV injection of contrast agent at cycle 7) was performed to determine BLB permeability. **(B)** Evolution of signal enhancement (mean  $\pm$  SE) along the DCE-MRI performed 72 h after LPS, in control (white circles,  $n = 16$ ), LPS (red circles,  $n = 16$ ), LPS plus SPT (green triangles,  $n = 14$ ) and LPS plus vehicle (orange triangles,  $n = 14$ ) experimental groups. **(C)** T1-weighted horizontal images acquired at DCE-MRI 30th cycle in representative rats from LPS + vehicle and LPS + SPT groups. A magnification of the cochlea is shown in the white square. **(D)** Signal enhancement (mean  $\pm$  SE) obtained in cycle 30th in the aforementioned experimental groups. Rats injected with LPS and treated with systemic dexamethasone for one (light blue,  $n = 9$ ) or three (dark blue,  $n = 5$ ) consecutive days after challenge, were also included. Statistically significant differences were calculated using one-way ANOVA ( $***p < 0.001$ , compared to controls;  $\#p < 0.05$ ,  $###p < 0.001$ , compared to LPS + vehicle). **(E)** ABR thresholds (mean  $\pm$  SE, in dB SPL) before and 72 h after LPS injection in rats treated with intratympanic SPT (green,  $n = 8$ ) or vehicle (orange,  $n = 11$ ). Statistically significant differences were calculated using the Mann-Whitney test ( $*p < 0.05$ )

more than 50% of the genes studied was elevated, including toll-like receptors (*Tlr2* and *Tlr3*), TLR4 signaling pathway cofactor (*Cd14*) and adaptor protein (*Myd88*), classical pro-inflammatory cytokines (*Il1a*, *Il6*, *Tnf* and *Il1r1*) and transcription factors (*Nfkb1*), among others. One hour after the second LPS challenge (time point 25 h), the expression of a limited set of genes including

*Il1b*, *Il10*, *Nfkbia* and *Ccl12* remained elevated. Finally, *Il18*, *Lyz2*, *Inf1a*, *Tlr4*, *Tlr5*, *Tlr9* and *Mpo* were overexpressed 72 h following LPS challenge (Fig. 6A).

We further studied several candidate genes selected from the array in control, LPS and LPS plus SPT-2101 treated rats 72 h after LPS challenge (Fig. 6B and Table 1). SPT-2101 pre-treatment normalized the expression of

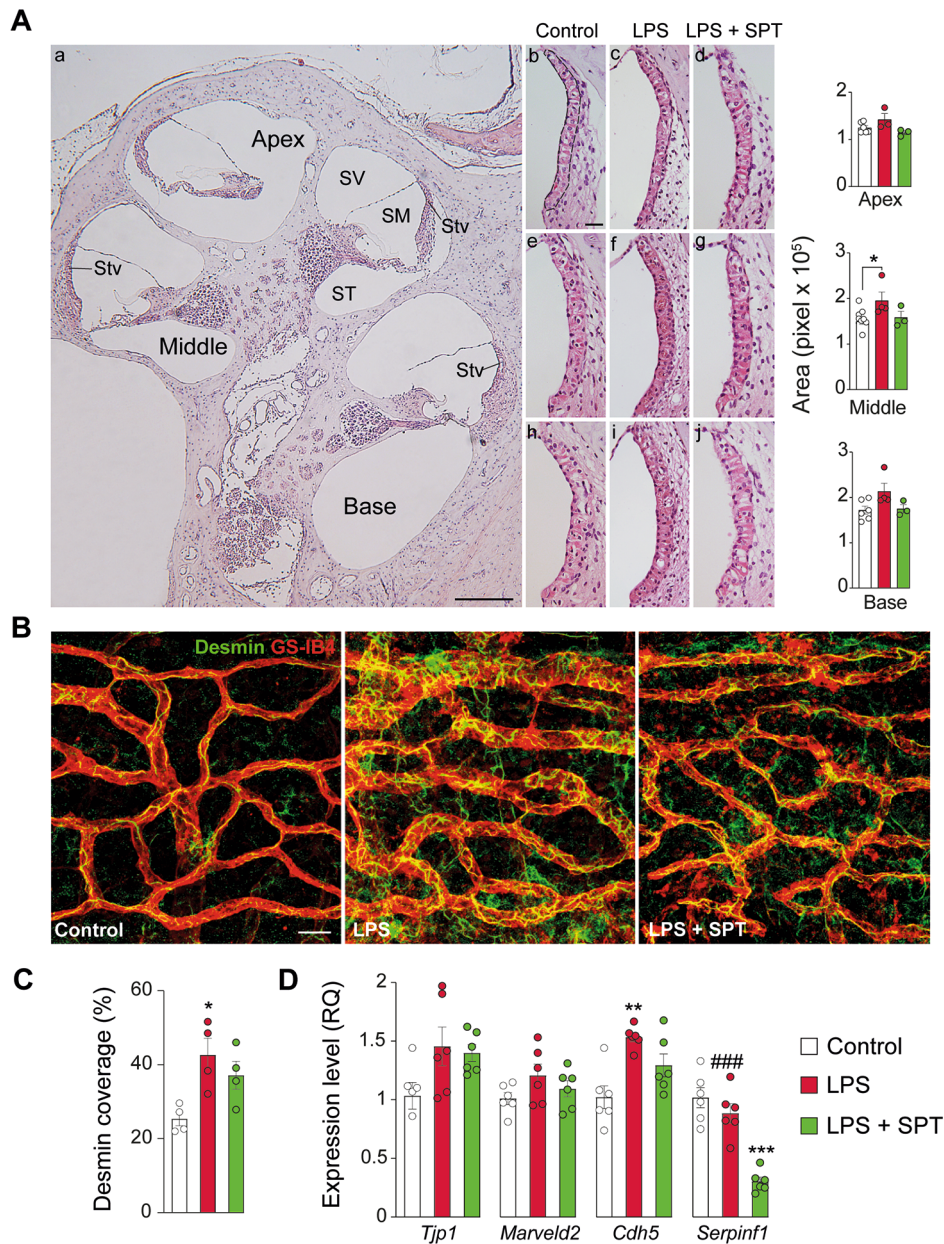


**Fig. 5** SPT-2101 protects the stria vascularis following LPS challenge. **(A)** Paraffin midmodiolar cochlear sections stained with hematoxylin-eosin. Representative image **(a)** showing the apical, middle and basal cochlear turns, the scala vestibuli (SV), tympanic (ST) and media (SM), and the stria vascularis (Stv) in each turn. Detail of the Stv in the apical **(b-d)**, middle **(e-g)** and basal **(h-j)** regions of control (white), LPS (red) and LPS plus SPT (green) rats, 72 h after challenge, and quantification of the strial area (outlined in **b**) (mean  $\pm$  SEM;  $n \geq 3$  rats per group, 10 measures per rat and region) in the right column. Paired comparisons were analyzed with the Mann-Whitney test (\* $p < 0.05$ , compared to control). Scale bar: 50 **(a)** and 10 **(b-j)**  $\mu\text{m}$ . **(B)** Representative confocal maximum projections of strial whole mounts showing capillaries (labeled with GS-IB4, in red) and pericytes branching (labeled with desmin, in green) in control, LPS and LPS plus SPT rats, 72 h after LPS injection. Scale bar: 25  $\mu\text{m}$ . **(C)** Desmin coverage of strial capillaries (%) assessed by desmin/GSIB4 co-localization. Values are presented as mean  $\pm$  SE ( $n = 4$  rats per group). **(D)** Expression level of tight-junction genes (*Tjp1*, *Cdh5* and *Marveld2*) and *Serpinf1* 72 h after LPS challenge, calculated as  $2^{-\Delta\Delta Ct}$  (RQ, mean  $\pm$  SE,  $n \geq 5$  rats per group), using *Tbp* as the reference gene and normalized to control rats. Statistical significance was analyzed by one-way ANOVA or the Kruskal-Wallis test (\* $p < 0.05$ ; \*\* $p < 0.01$ ; \*\*\* $p < 0.001$ , compared to control; ### $p < 0.001$ , compared to LPS).

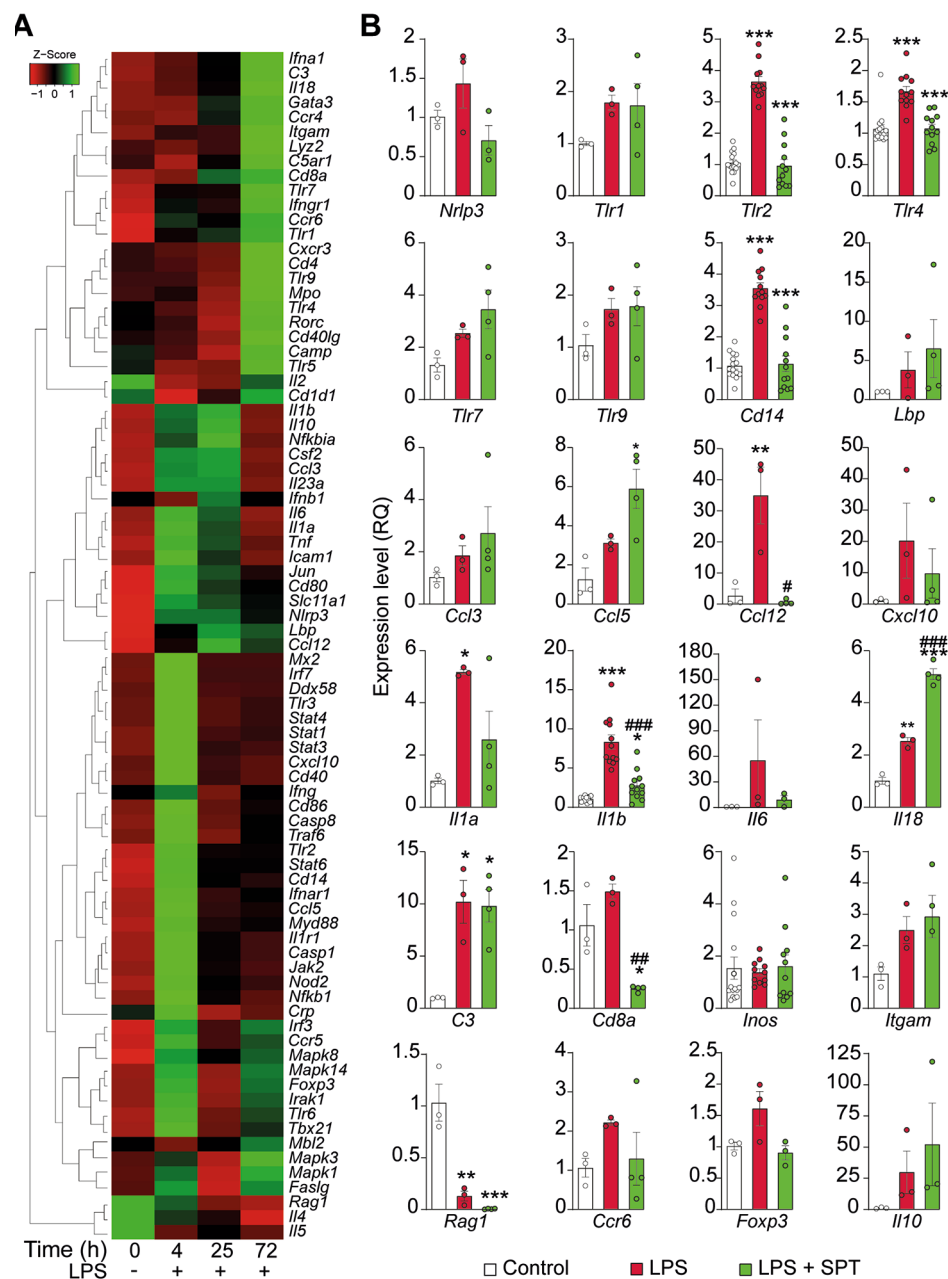


**Fig. 6** SPT-2101 prevents LPS-induced alterations of cochlear immune and inflammatory response transcripts. **(A)** Heatmap representation of PCR array expression data ( $2^{-\Delta C_t}$ ) from control or LPS-injected rats, 4, 25 and 72 h after injection. At least 3 cochleae from different rats per group were studied. **(B)** RT-qPCR expression levels of candidate genes selected from A in control (white), LPS (red) or LPS plus SPT (green) experimental groups, 72 h after the first LPS injection. Results were calculated as  $2^{-\Delta\Delta C_t}$  (RQ, expressed as mean  $\pm$  SE), using *Tbp* as the reference gene and normalized to control rats without LPS. At least 3 rats were included for each group. Statistical significance was analyzed by either one-way ANOVA or the Kruskal-Wallis test (\* $p < 0.05$ ; \*\* $p < 0.01$ ; \*\*\* $p < 0.001$  compared to controls; ## $p < 0.01$ , ### $p < 0.001$  compared to LPS).

toll-like receptors (*Tlr2* and *Tlr4*), the LPS-response gene *Cd14*, pathogen-associated molecular pattern recognition receptor *Nlrp3* and cytokines (*Ccl12* and *Il1b*), among others. These data suggest that the observed protection of BLB integrity provided by SPT-2101 occurs, at least partly, at the transcriptional level, by reducing the expression of LPS receptors and inflammatory genes.

#### SPT-2101 reduces the number of activated macrophages in the cochlea after lipopolysaccharide challenge

LPS challenge induced a significant increase in the levels of macrophage marker IBA1 in the spiral ligament and spiral ganglion along the cochlea (basal, middle and apical regions). Of note, IBA1 reactivity was significantly lower in rats pre-treated with SPT-2101 than in

**Table 1** Expression levels of immune response genes in SPT-2101 treated rats. Genes were selected from those included in the RT<sup>2</sup>-Profiler™ PCR Array Rat Innate & Adaptive Immune Responses and represented in Fig. 6A. RT-qPCR expression levels of selected genes in LPS and LPS plus SPT-2101 experimental groups (n ≥ 3 rats per experimental condition), 72 h after the first LPS injection. Results were calculated as 2<sup>-ΔΔCt</sup> (RQ expressed as mean ± SEM), using *Tbp* as the reference gene, and normalized to control rats without LPS. Column on the right shows fold-change between LPS-challenged rats treated or not with SPT-2101. In bold, fold changes > 1 and < -0.5

Category	Gene	Expression level (RQ ± SEM)		SPT-2101 vs. LPS Fold-change
		LPS	LPS + SPT-2101	
Pattern Recognition Receptors	<i>Mip3</i>	1.434 ± 0.313	0.709 ± 0.191	<b>-0.506</b>
	<i>Thr1</i>	1.788 ± 0.142	1.731 ± 0.418	-0.032
	<i>Thr2</i>	3.645 ± 0.161	0.960 ± 0.207	<b>-0.736</b>
	<i>Thr4</i>	1.667 ± 0.079	1.074 ± 0.069	-0.355
	<i>Thr7</i>	2.544 ± 0.153	3.451 ± 0.741	0.357
	<i>Thr9</i>	1.728 ± 0.206	1.786 ± 0.375	0.034
	<i>Ccl3</i>	1.856 ± 0.376	2.712 ± 1.012	0.462
	<i>Ccl5</i>	3.121 ± 0.204	5.886 ± 1.000	0.886
	<i>Ccl12</i>	34.920 ± 9.145	0.590 ± 0.389	<b>-0.983</b>
	<i>Cxcl10</i>	20.243 ± 11.997	9.785 ± 7.904	<b>-0.517</b>
Cytokines	<i>Il1a</i>	5.179 ± 0.094	2.590 ± 1.088	<b>-0.500</b>
	<i>Il1b</i>	8.328 ± 0.921	2.758 ± 0.533	-0.668
	<i>Il6</i>	55.325 ± 47.534	9.258 ± 4.617	<b>-0.833</b>
	<i>Il18</i>	2.530 ± 0.140	5.094 ± 0.208	<b>1.013</b>
	<i>Cd14</i>	3.551 ± 0.173	1.138 ± 0.254	<b>-0.679</b>
	<i>Lbp</i>	3.781 ± 2.305	6.519 ± 3.698	0.724
	<i>Foxp3</i>	1.609 ± 0.274	0.905 ± 0.111	-0.437
	<i>Il10</i>	29.825 ± 17.028	52.233 ± 33.181	0.751
	<i>Ccr6</i>	2.218 ± 0.065	1.293 ± 0.674	-0.417
	<i>C3</i>	10.199 ± 2.051	9.808 ± 1.543	-0.038
Other Inflammatory-related genes	<i>Cd8a</i>	1.492 ± 0.095	0.249 ± 0.019	<b>-0.833</b>
	<i>iNos</i>	1.380 ± 0.138	1.611 ± 0.437	0.167
	<i>Itgam</i>	2.499 ± 0.429	2.929 ± 0.678	0.172
Treg Markers	<i>Rag1</i>	0.129 ± 0.048	0.005 ± 0.002	<b>-0.960</b>
Response to LPS				
Treg Markers				
Th17 Markers				

vehicle-treated rats before LPS-challenge (Fig. 7A–C), further confirming the anti-inflammatory actions of SPT-2101 and protection against LPS.

To explore the potential molecular targets of SPT-2101, we determined the cochlear protein levels of NOD-like receptor family, pyrin domain-containing 3 (NLRP3), an important inflammasome sensor molecule, and of nuclear factor erythroid 2-related factor (NRF2), a critical defense element against oxidative stress [40, 41]. Western blotting of cochlear protein samples revealed higher levels of NLRP3 and NRF2 in LPS-challenged rats than in control rats, consistent with the activation of the inflammasome and antioxidant responses. Notably, animals pre-treated with SPT-2101 showed decreased levels of both proteins (Fig. 7D).

## Discussion

Inflammation is a common pathogenic mechanism in auditory pathology and accordingly, anti-inflammatories, mostly corticosteroids, have been used to revert this process [30, 42]. Cochlear inflammation involves changes in BLB permeability and in the last decade, it has been shown that BLB dysfunction can contribute to the development of sensorineural hearing loss of different etiologies [2, 25, 26, 43]. In the present study, we demonstrate the therapeutic efficacy of a new dexamethasone formulation for intratympanic administration, SPT-2101, in an *in vivo* model of endotoxemia-induced inflammation. Our results show that SPT-2101 suppresses inflammatory response in the cochlea and normalizes BLB permeability in LPS-challenged rats.

Systemic administration of LPS has been extensively used to model cochlear inflammation and BLB alterations. This involves resident macrophage activation, ultimately leading to inner ear inflammation (labyrinthitis), BLB disruption and hearing loss [19, 44]. LPS-induced BLB disruption and leakage varies from mild to severe depending on the species, exposure route (local vs. systemic) and concentration of LPS [11]. Administration of LPS directly into the scala media of guinea pigs, an experimental model of immune-mediated Meniere's disease, induced severe hydrops, immune cell infiltration, and permanent hearing loss [11]. LPS-induced hearing loss is not generally associated with hair cell loss [45]. Indeed, loss of the endocochlear potential due to perturbation of vascular permeability and ion transport in the stria vascularis is considered as the main cause of LPS-induced hearing thresholds shifts [14, 19]. Accordingly, in the present study, we found no hair cell loss or signs of synaptopathy, suggesting that ABR threshold shifts were due to the impact of LPS challenge on BLB permeability, causing leakage and altered endolymph homeostasis.

Here, we performed a longitudinal study of LPS-induced alterations in the vascular permeability of the

cochlea with DCE-MRI. Previous preclinical and clinical studies confirm the association between increase in gadolinium uptake and loss of BLB integrity [23, 24, 46].

The first changes in the DCE-MRI pattern were apparent 1 h after LPS injection and were clearly observable 4 h after LPS challenge. The second LPS injection potentiated the increase in signal enhancement, which was maintained along the following 48 h, with significant differences compared with control animals. These results are similar to those reported in guinea pigs receiving LPS and imaged by MRI at 4–10 days after challenge [24]. Our results offer novel insight into the short-term dynamics of BLB permeability and indicate an early impact in the first hours following LPS challenge.

We found that the changes in BLB permeability induced by LPS were accompanied by transitory shifts in inflammatory gene expression, with the majority of the analyzed transcripts showing a rapid increase in expression after the first and/or the second LPS injection, and decreasing thereafter. These included the canonical LPS-recognizing receptor *Tlr4* and cofactor *Cd14*, but also other toll-like receptors such as *Tlr1*, 2, 5, 6, 7 and 9. TLR2 is not the canonical LPS-recognizing receptor, but it is required for LPS-induced TLR4 signaling in some tissues [39]. Interestingly, we observed an early increase in *Tlr2* and *Cd14* 4 h after LPS, whereas *Tlr4* expression increased at 72 h after challenge.

Besides, LPS induced an upregulation of classical pro-inflammatory cytokines (*Il1b*, *Il6*, *Tnf*) and *Inos*, which showed a robust increase in expression ( $\approx 100$ -fold) 2 h after LPS challenge. Auditory cells produce nitric oxide in response to bacterial LPS, and inhibition of iNOS reduces cochlear injury [47–49].

Transforming growth factor-beta 1 has a key role in the regulation of the immune response, especially immunosuppressive effects, along with IL10. Several studies confirm that TGFB inhibits LPS inflammatory response through suppression of inflammatory cytokines expression in macrophages [50]. Here we observed that *Tgfb* expression also increases in the cochlea 1–2 days after LPS challenge. Similarly, we previously found an increase in the cochlear expression of *Tgfb1* and *TgfbR1* along with a decrease in *Tgfb2* and *TgfbR2* gene expression 24 h after noise exposure [51]. Therefore, our results confirm in different models of cochlear damage an increase in the expression of TGF elements in the first hours after insult, which could indicate the initiation of the immunosuppressive response.

Like TGFB, FOXP3 is considered a regulator of transcription in T cells, playing a suppressive role in the immune response [52], although *Foxp3* has been reported to be also expressed by other lymphoid or myeloid cells, as well as by non-hematopoietic cells, such as epithelial cells. Cochlear resident macrophages stimulate the

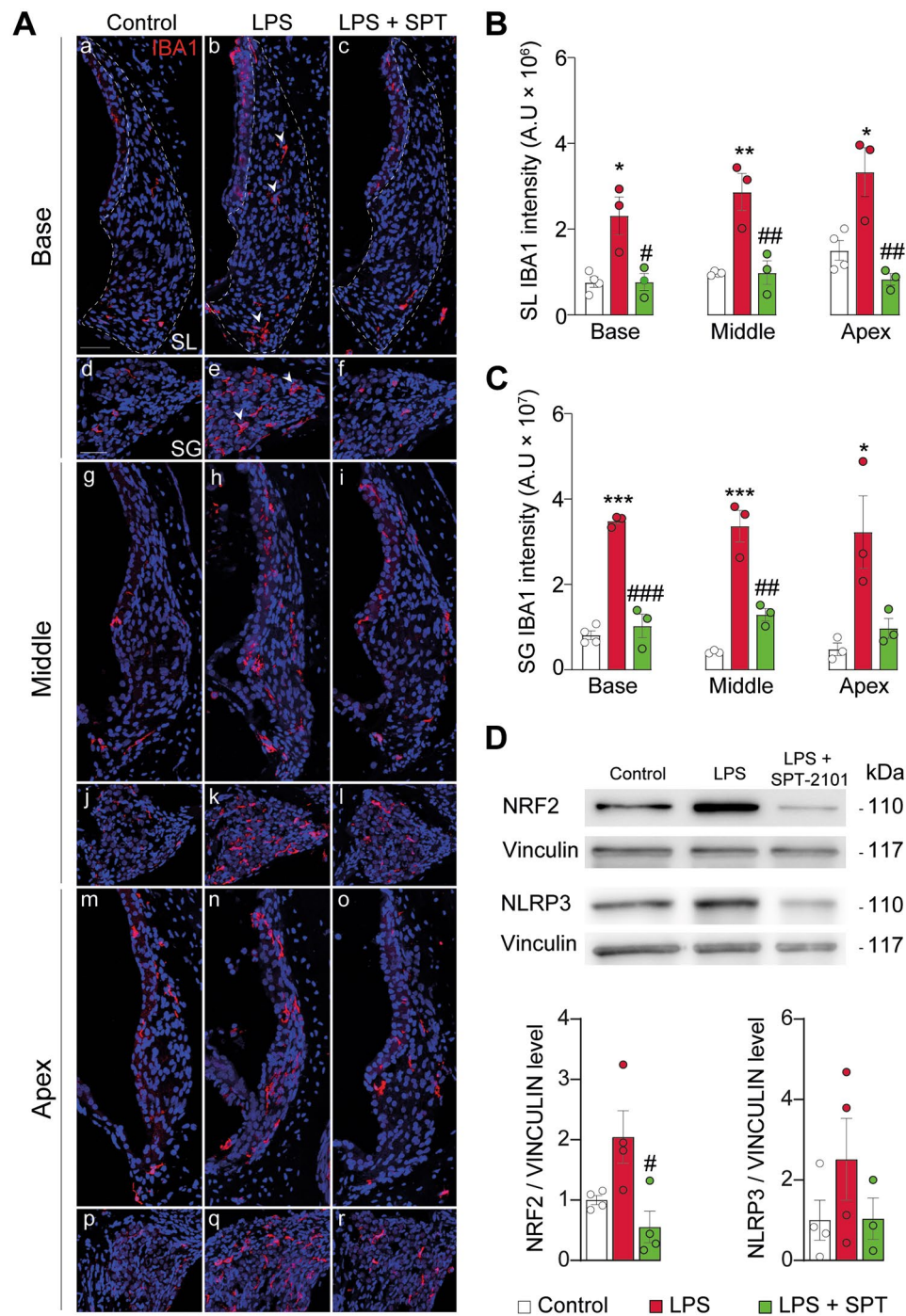


**Fig. 7** SPT-2101 treatment reduces macrophage infiltration and oxidative stress after LPS challenge. **(A)** Representative confocal maximum projections of cochlear cross-cryosections immunolabeled for IBA1 (in red), showing the spiral ligament (SL, outlined in a–c) and spiral ganglion (SG) of basal (a–f), middle (g–l) and apical (m–r) cochlear turns of control, LPS and LPS plus SPT groups, 72 h after LPS challenge. White arrowheads highlight positive staining of macrophages. Scale bar: 50  $\mu$ m. **(B)** and **(C)** IBA1 total staining intensity quantification in the SL **(B)** and SG **(C)**, in control (white), LPS (red), and LPS plus SPT (green) experimental groups. Values are presented as mean  $\pm$  SE, from at least 3 rats per group. Statistical significance was analyzed by either one-way ANOVA or the Kruskal-Wallis test (\* $p < 0.05$ ; \*\* $p < 0.01$ ; \*\*\* $p < 0.001$ , compared to control; # $p < 0.05$ ; ## $p < 0.01$ ; ### $p < 0.001$ , compared to LPS). **(D)** Western blotting of whole cochlea protein extracts from control, LPS and LPS + SPT groups, 4 h after LPS injection. NLRP3 and NRF2 levels are relative to those of vinculin, and normalized to those from control rats. Data presented as mean  $\pm$  SE,  $n = 4$  rats per condition. Statistical significance was analyzed by ANOVA (# $p < 0.05$ , compared to LPS).

infiltration of other immune cells, as B and T lymphocytes, NK cells, monocytes and neutrophils, in response to injury [53]. Indeed, there are evidences pointing to cochlear infiltration of CD4+CD25+regulatory T cells associated to transcription of *Foxp3* following rat immunization with myelin protein zero, an experimental model of a human autoimmune disease causing deafness [54]. Accordingly, increased *Foxp3* and *Il10* expression has been reported in the *Dusp1* knock out, which shows chronic cochlear inflammation and premature age-related hearing loss [34, 54]. Here we show the increase in the cochlear expression levels of *Foxp3* following each LPS challenge, supporting that FOXP3 role is to suppress immune cell responses by inducing the expression of immunosuppressive cytokines, such as IL-10.

In short, LPS induces a series of sequential changes in inflammatory gene expression, possibly due to the successive participation of different cell types in the immune response, including resident macrophages, recruited monocytes and neutrophils, as well as perivascular melanocytes and fibrocytes. Our gene expression analysis updates and extends recent research aimed to better understand the molecular mechanisms involved in the response to LPS-induced endotoxemia [55].

LPS specially affects tight junctions in the blood-labyrinth barrier. In addition to induce a down-regulation of tight junction associated proteins ZO-1, occludin, and VE-cadherin in endothelial cells [16, 17], LPS also causes an increase in MMP-9 levels produced by perivascular macrophages [17]. MMP-9 degrades extracellular matrix components and damages the tight junctions and vascular basement membrane, leading to BLB breakdown. Of note, inhibition of MMP-9 with oxytetracycline and ilomastat was found to ameliorate BLB breakdown in guinea pigs challenged with intratympanic instillation of LPS [18]. We found that LPS-challenged rats had elevated cochlear expression of *Tjp1*, *Marveld2* and *Cdh5*, which promote the synthesis of the tight junction proteins ZO-1, tricellulin and VE-cadherin, respectively. This finding suggests the presence of a feedback compensation circuit for MMP-9-induced degradation. We found that LPS challenge increased ABR thresholds and BLB leakage, with the consequent impact on endolymph homeostasis, but no cell loss or signs of synaptopathy.

The characterization of cellular and molecular alterations in the cochlea following LPS challenge have guided the identification of potential molecular targets and aided in the development of novel treatments, including peroxisome proliferator-activated receptor gamma agonists, NLRP3 and iNOS inhibitors, IL-1 receptor antagonists or small interference RNAs, among others [40, 48, 56, 57]. However, as inflammation is the main pathological process in LPS-induced inner ear damage, anti-inflammatory

drugs (mainly corticosteroids) remain the cornerstone of treatment.

Dexamethasone is an extensively used synthetic glucocorticoid for its anti-inflammatory and immunosuppressive effects in the cochlea [30], where glucocorticoid receptors have been identified in the stria vascularis, spiral ligament, auditory ganglion and organ of Corti [31]. On one hand, dexamethasone is currently used in clinical practice to treat sudden idiopathic hearing loss, acute noise-induced hearing loss and Meniere's disease [58–60]. On the other hand, its use in bacterial otitis is controversial, especially when administered systemically [61, 62]. Systemic dexamethasone administration causes adverse effects including hypertension, peptic ulcers, hyperglycemia, and hydro-electrolytic disorders [63]. This has fostered interest in the development of novel dexamethasone-loaded nanoformulations that achieve sustained drug delivery with a single administration to improve efficacy and reduce adverse effects.

Here we demonstrate the therapeutic effect of SPT-2101, a new dexamethasone formulation for intratympanic administration whereby the glucocorticoid is combined with a trilycine and polyethylene glycol. This in situ-forming hydrogel impairs clearing from the middle ear after injection and allows a sustained delivery, avoiding SPT-2101 novel repeated intratympanic administrations.

We administered SPT-2101 to rats prior to systemic LPS challenge, observing a notable reduction in MRI signal enhancement with respect to vehicle-treated rats. Indeed, SPT-2101-treated rats had a DCE-MRI profile similar to control non LPS-challenged rats. The SPT-2101 formulation administered in a single middle ear injection maintained BLB integrity and conferred protection comparable with that of systemic dexamethasone administration over three consecutive days, supporting the importance of local dexamethasone treatment as an effective and safe therapeutic option to reduce the adverse effects associated with systemic treatments. In agreement with the MRI results, ABR data showed preserved hearing in rats treated with SPT-2101, especially for high frequencies.

As the increased vascular permeability is likely due to loss of BLB integrity, we hypothesized that SPT-2101 protected the stria vascularis. LPS triggered an enlargement of the stria vascularis, accompanied by dilatation of capillaries and alterations in pericytes, which was sufficient to disrupt BLB integrity. These changes were not observed in rats pre-treated with SPT-2101. Moreover, *Serpinf1* levels were significantly lower in rats treated with SPT-2101 than in untreated LPS-challenged rats. Pigment epithelium-derived factor (PEDF), also known as SERPINF1, is a broadly expressed protein with critical roles in many physiological and pathological processes,



including neuroprotection, angiogenesis, fibrogenesis and inflammation, and it is a potent endogenous inhibitor of vascular permeability in the retina and brain [64]. PEDF has been identified in the basilar membrane, in the spiral ganglion neurons and in the blood vessels in the stria vascularis, although its role in the cochlea is not well defined. Perivascular macrophages modulate the expression of ZO-1 and VE-cadherin through secretion of PEDF, and changes in *Serpinf1* expression have been described in response to different cochlear insults. Zhang et al. reported that noise exposure in mice caused BLB hyperpermeability associated with suppressed PEDF production. Accordingly, delivery of PEDF to the injured ear recovered BLB integrity and hearing thresholds [25]. Our data suggest that SPT-2101 may promote similar protective mechanisms in the LPS-challenged cochlea.

At the molecular level, SPT-2101 counteracted the changes in the expression of inflammatory genes 72 h after LPS injection, especially the toll-like receptors *Tlr2*, *Tlr4* and cofactor *Cd14*, as well as *Nlrp3*. NLRP3 inflammasome activation associates with hearing loss both of genetic and induced etiology [65, 66]. SPT-2101 treatment normalized the expression of cytokines and other inflammatory-related genes, including *Il1b*, *Il18*, *Ccl12*, *Cd8a* and *Rag1*. SPT-2101-treated rats also maintained the protein levels of NRF2 and NLRP3, two key modulators of inflammatory and stress responses [40, 41]. Pro-inflammatory cytokines are involved in chemotaxis and immune cell infiltration, which is common following LPS exposure [45]. Accordingly, SPT-2101 reduced infiltration of IBA1+ macrophages in the lateral wall, specifically in the type IV fibrocyte area of the spiral ligament, as well as in the spiral ganglion.

## Conclusions

A novel dexamethasone nanoformulation SPT-2101 prevents LPS-driven otic inflammation-related events, including cytokine and proinflammatory signals gene expression, BLB disruption, and immune cell recruitment and infiltration. A single administration by intratympanic injection of SPT-2101 sufficed to protect BLB integrity and maintained hearing thresholds, in striking contrast with the lower efficacy shown by dexamethasone administered systemically. Local administration of dexamethasone formulated as SPT-2101 thus offers a novel therapeutic opportunity to treat diseases related to BLB dysfunction.

## Abbreviations

ABR	Auditory Brainstem Response
BLB	Blood-labyrinth barrier
DCE-MRI	Dynamic contrast-enhanced magnetic resonance imaging
IHC	Inner hair cell
LPS	Lipopolysaccharide
OHC	Outer hair cell

## Acknowledgements

We acknowledge our colleagues at the Neuropathology of Hearing and Myelinopathies Group for technical support and critical comments. We also thank the Non-Invasive Neurofunctional Evaluation and Genomic facilities (Institute for Biomedical Research "Alberto Sols" CSIC-UAM) and the Histology facility (National Biotechnology Center, CSIC) for technical support. We dedicate this work to the memory of our colleague and friend Prof. Sebastian Cerdán.

## Authors' contributions

SM-C, conceptualization, investigation, data analysis, writing original draft, writing review and editing; IV-N, conceptualization, data analysis, supervision, project administration, funding acquisition, writing review and editing; EL, JMB, ET and LR-dLR, investigation, data analysis and writing methods; PL and SE, data analysis, writing review and editing. All authors have read and approved the manuscript.

## Funding

This work was funded by a CIBERER-ISCIi SPIRALTH-CIBERER ER17PE12 and MICINN/AEI PID2020-115274RB-I00 grants to IVN and SMC and with the support of Comunidad de Madrid MINA-CM P2022-BMD-7236 and COST Action CA20121 BedBenPhar. Open Access funding provided by Consejo Superior de Investigaciones Científicas. SMC, EL, JMB and LRR held CIBERER contracts.

Open Access funding provided thanks to the CRUE-CSIC agreement with Springer Nature.

## Data Availability

The datasets generated and/or analyzed during the current study are available in the Digital CSIC repository at <https://doi.org/10.20350/digitalCSIC/15167>.

## Declarations

### Ethics approval and consent to participate

All animal experimental procedures followed European Community 2010/63/EU and Spanish RD 53/2013 guidelines with the corresponding authorization from the competent authority (PROEX 256/19 and 325.4/21).

### Consent for publication

Not Applicable.

### Competing interests

SMC, IVN, JMB and EL have received research support from Spiral Therapeutics, and SE was working at Spiral Therapeutics. These competing financial and professional interests have not influenced the work described in this manuscript.

### Author details

<sup>1</sup>Institute for Biomedical Research Sols-Morreale, Spanish National Research Council- Autonomous University of Madrid (CSIC-UAM), Madrid 28029, Spain

<sup>2</sup>Centre for Biomedical Network Research on Rare Diseases (CIBERER), Institute of Health Carlos III (ISCIII), Madrid 28029, Spain

<sup>3</sup>Hospital La Paz Institute for Health Research (IdiPAZ), Madrid 28029, Spain

<sup>4</sup>Spiral Therapeutics, Inc, South San Francisco, CA, USA

Received: 22 May 2023 / Accepted: 29 September 2023

Published online: 11 October 2023

## References

1. Neng L, Zhang F, Kachelmeier A, Shi X. Endothelial cell, pericyte, and perivascular resident macrophage-type melanocyte interactions regulate cochlear intrastrial fluid-blood barrier permeability. *J Assoc Res Otolaryngol*. 2013;14:175–85. <https://doi.org/10.1007/s10162-012-0365-9>.
2. Shi X. Pathophysiology of the cochlear intrastrial fluid-blood barrier (review). *Hear Res*. 2016;338:52–63. <https://doi.org/10.1016/j.heares.2016.01.010>.

3. Perin P, Marino F, Varela-Nieto I, Szczepek AJ, Editorial. Neuroimmunology of the inner ear. *Front Neurol* 2021;12.
4. Keithley EM. Inner ear immunity. *Hear Res.* 2022;419:108518. <https://doi.org/10.1016/j.heares.2022.108518>.
5. Cai Q, Vethanayagam RR, Yang S, Bard J, Jamison J, Cartwright D, et al. Molecular profile of cochlear immunity in the resident cells of the organ of Corti. *J Neuroinflammation.* 2014;11:173. <https://doi.org/10.1186/s12974-014-0173-8>.
6. Milon B, Shulman ED, So KS, Cederroth CR, Lipford EL, Sperber M, et al. A cell-type-specific atlas of the inner ear transcriptional response to acoustic trauma. *Cell Rep.* 2021;36:109758. <https://doi.org/10.1016/j.celrep.2021.109758>.
7. Zhang W, Dai M, Fridberger A, Hassan A, Degagne J, Neng L, et al. Perivascular-resident macrophage-like melanocytes in the inner ear are essential for the integrity of the intrastrial fluid-blood barrier. *Proc Natl Acad Sci U S A.* 2012;109:10388–93. <https://doi.org/10.1073/pnas.1205210109>.
8. Zhang F, Zhang J, Neng L, Shi X. Characterization and inflammatory response of perivascular-resident macrophage-like melanocytes in the vestibular system. *J Assoc Res Otolaryngol.* 2013;14:635–43. <https://doi.org/10.1007/s10162-013-0403-2>.
9. Bae SH, Yoo JE, Choe YH, Kwak SH, Choi JY, Jung J, et al. Neutrophils infiltrate into the spiral ligament but not the stria vascularis in the cochlea during lipopolysaccharide-induced inflammation. *Theranostics.* 2021;11:2522–33. <https://doi.org/10.7150/thno.49121>.
10. Quintanilla-Dieck L, Larrain B, Trune D, Steyger PS. Effect of systemic lipopolysaccharide-induced inflammation on cytokine levels in the murine cochlea: a pilot study. *Otolaryngol Head Neck Surg.* 2013;149:301–3. <https://doi.org/10.1177/0194599813491712>.
11. Brown DJ, Sokolic L, Fung A, Pastras CJ. Response of the inner ear to lipopolysaccharide introduced directly into scala media. *Hear Res.* 2018;370:105–12. <https://doi.org/10.1016/j.heares.2018.10.007>.
12. Ciesielska A, Matyjek M, Kwiatkowska K. TLR4 and CD14 trafficking and its influence on LPS-induced pro-inflammatory signaling. *Cell Mol Life Sci.* 2021;78:1233–61. <https://doi.org/10.1007/s00018-020-03656-y>.
13. Hough K, Verschuur CA, Cunningham C, Newman TA. Macrophages in the cochlea; an immunological link between risk factors and progressive hearing loss. *Glia.* 2022;70:219–38. <https://doi.org/10.1002/glia.24095>.
14. Hirose K, Li S-Z, Ohlemiller KK, Ransohoff RM. Systemic lipopolysaccharide induces cochlear inflammation and exacerbates the synergistic ototoxicity of kanamycin and furosemide. *J Assoc Res Otolaryngol.* 2014;15:555–70. <https://doi.org/10.1007/s10162-014-0458-8>.
15. Hirose K, Hartsock JJ, Johnson S, Santi P, Salt AN. Systemic lipopolysaccharide compromises the blood-labyrinth barrier and increases entry of serum fluorescein into the perilymph. *J Assoc Res Otolaryngol.* 2014;15:707–19. <https://doi.org/10.1007/s10162-014-0476-6>.
16. Zhang J, Chen S, Hou Z, Cai J, Dong M, Shi X. Lipopolysaccharide-induced middle ear inflammation disrupts the cochlear intra-strial fluid-blood barrier through down-regulation of tight junction proteins. *PLoS ONE.* 2015;10:e0122572. <https://doi.org/10.1371/journal.pone.0122572>.
17. Jiang Y, Zhang J, Rao Y, Chen J, Chen K, Tang Y. Lipopolysaccharide disrupts the cochlear blood-labyrinth barrier by activating perivascular resident macrophages and up-regulating MMP-9. *Int J Pediatr Otorhinolaryngol.* 2019;127:109656. <https://doi.org/10.1016/j.ijporl.2019.109656>.
18. Choi CH, Jang CH, Cho YB, Jo SY, Kim MY, Park BY. Matrix metalloproteinase inhibitor attenuates cochlear lateral wall damage induced by intratympanic instillation of endotoxin. *Int J Pediatr Otorhinolaryngol.* 2012;76:544–8. <https://doi.org/10.1016/j.ijporl.2012.01.013>.
19. Hirose K, Li S-Z. The role of monocytes and macrophages in the dynamic permeability of the blood-perilymph barrier. *Hear Res.* 2019;374:49–57. <https://doi.org/10.1016/j.heares.2019.01.006>.
20. Juhn SK, Jung M-K, Hoffman MD, Drew BR, Preciado DA, Sausen NJ, et al. The role of inflammatory mediators in the pathogenesis of otitis media and sequelae. *Clin Exp Otorhinolaryngol.* 2008;1:117–38. <https://doi.org/10.3342/ceo.2008.1.3.117>.
21. Koo J-W, Quintanilla-Dieck L, Jiang M, Liu J, Urdang ZD, Allensworth JJ, et al. Endotoxemia-mediated inflammation potentiates aminoglycoside-induced ototoxicity. *Sci Transl Med.* 2015;7:298ra118. <https://doi.org/10.1126/scitranslmed.aac5546>.
22. Oh G-S, Kim H-J, Choi J-H, Shen A, Kim C-H, Kim S-J, et al. Activation of lipopolysaccharide-TLR4 signaling accelerates the ototoxic potential of cisplatin in mice. *J Immunol.* 2011;186:1140–50. <https://doi.org/10.4049/jimmunol.1002183>.
23. Song CI, Pogson JM, Andresen NS, Ward BK. MRI with Gadolinium as a measure of blood-labyrinth Barrier Integrity in patients with inner ear symptoms: a scoping review. *Front Neurol.* 2021;12:662264. <https://doi.org/10.3389/fneur.2021.662264>.
24. Floc'h JL, Tan W, Telang RS, Vljakovic SM, Nuttall A, Rooney WD, et al. Markers of cochlear inflammation using MRI. *J Magn Reson Imaging.* 2014;39:150–61. <https://doi.org/10.1002/jmri.24144>.
25. Zhang F, Dai M, Neng L, Zhang JH, Zhi Z, Fridberger A, et al. Perivascular macrophage-like melanocyte responsiveness to acoustic trauma—a salient feature of stria barrier associated hearing loss. *FASEB J.* 2013;27:3730–40. <https://doi.org/10.1096/fj.13-232892>.
26. Neng L, Zhang J, Yang J, Zhang F, Lopez IA, Dong M, et al. Structural changes in the stria barrier of aged C57BL/6 mice. *Z Für Zellforschung Und Mikroskopische Anatomie (Vienna Austria: 1948).* 2015;361:685–96. <https://doi.org/10.1007/s00441-015-2147-2>.
27. Miwa T, Okano T. Role of inner ear macrophages and Autoimmune/Autoinflammatory mechanisms in the pathophysiology of inner ear disease. *Front Neurol.* 2022;13:861992. <https://doi.org/10.3389/fneur.2022.861992>.
28. Cohen-Salmon M, Regnault B, Cayet N, Caille D, Demuth K, Hardelin J-P, et al. Connexin30 deficiency causes intrastrial fluid-blood barrier disruption within the cochlear stria vascularis. *Proc Natl Acad Sci U S A.* 2007;104:6229–34. <https://doi.org/10.1073/pnas.0605108104>.
29. Kalinec GM, Lomber G, Urrutia RA, Kalinec F. Resolution of cochlear inflammation: Novel Target for preventing or ameliorating Drug-, noise- and age-related hearing loss. *Front Cell Neurosci.* 2017;11:192. <https://doi.org/10.3389/fncel.2017.00192>.
30. Magdalena B, Skarzynska, Piotr H. In: Celso, Pereira, Corticosteroids, editors. *Skarzynski. Corticosteroids in Otorhinolaryngology.* Rijeka: IntechOpen; 2021. Ch. 3. <https://doi.org/10.5772/intechopen.98636>.
31. Terakado M, Kumagami H, Takahashi H. Distribution of glucocorticoid receptors and 11 beta-hydroxysteroid dehydrogenase isoforms in the rat inner ear. *Hear Res.* 2011;280:148–56. <https://doi.org/10.1016/j.heares.2011.05.006>.
32. Heywood RL, Ifeacho SN, Narula AA. Effect of intratympanic steroid administration on sensorineural hearing loss associated with acute otitis media. *J Laryngol Otol.* 2016;130:532–5. <https://doi.org/10.1017/S0022215116001110>.
33. Murillo-Cuesta S, Celaya AM, Cervantes B, Bermúdez-Muñoz JM, Rodríguez-de la Rosa L, Contreras J, et al. Therapeutic efficiency of the APAF-1 antagonist LPT99 in a rat model of cisplatin-induced hearing loss. *Clin Transl Med.* 2021;11:e363. <https://doi.org/10.1002/ctm2.363>.
34. Celaya AM, Sánchez-Pérez I, Bermúdez-Muñoz JM, Rodríguez-de la Rosa L, Pintado-Berniches L, Perona R et al. Deficit of mitogen-activated protein kinase phosphatase 1 (DUSP1) accelerates progressive hearing loss. *Elife* 2019;8. <https://doi.org/10.7554/eLife.39159>.
35. Bermúdez-Muñoz JM, Celaya AM, Hijazo-Pechero S, Wang J, Serrano M, Varela-Nieto I. G6PD overexpression protects from oxidative stress and age-related hearing loss. *Aging Cell.* 2020;19:e13275. <https://doi.org/10.1111/acer.13275>.
36. Liberman MC, Liberman LD, Maison SF. Efferent feedback slows cochlear aging. *J Neurosci.* 2014;34:4599–607. <https://doi.org/10.1523/JNEUROSCI.4923-13.2014>.
37. Sanchez-Calderon H, Rodriguez-de la Rosa L, Milo M, Pichel JG, Holley M, Varela-Nieto I. RNA microarray analysis in prenatal mouse Cochlea reveals novel IGF-I target genes: implication of MEF2 and FOXM1 transcription factors. *PLoS ONE.* 2010;5:e8699. <https://doi.org/10.1371/journal.pone.0008699>.
38. Babicki S, Arndt D, Marcu A, Liang Y, Grant JR, Maciejewski A, et al. Heatmapper: web-enabled heat mapping for all. *Nucleic Acids Res.* 2016;44:W147–53. <https://doi.org/10.1093/nar/gkw419>.
39. Good DW, George T, Watts BA. Toll-like receptor 2 is required for LPS-induced toll-like receptor 4 signaling and inhibition of ion transport in renal thick ascending limb. *J Biol Chem.* 2012;287:20208–20. <https://doi.org/10.1074/jbc.M111.336255>.
40. Ma J-H, Lee E, Yoon S-H, Min H, Oh JH, Hwang I, et al. Therapeutic effect of NLRP3 inhibition on hearing loss induced by systemic inflammation in a CAPS-associated mouse model. *EBioMedicine.* 2022;82:104184. <https://doi.org/10.1016/j.ebiom.2022.104184>.
41. Panda H, Wen H, Suzuki M, Yamamoto M. Multifaceted roles of the KEAP1-NRF2 system in Cancer and Inflammatory Disease Milieu. *Antioxid (Basel).* 2022;11:538. <https://doi.org/10.3390/antiox11030538>.
42. Windsor AM, Ruckenstein MJ. Anti-inflammatory therapies for Sensorineural hearing loss. In: Ramkumar V, Rybak LP, editors. *Inflammatory mechanisms in mediating hearing loss.* Cham: Springer International Publishing; 2018. pp. 189–210. [https://doi.org/10.1007/978-3-319-92507-3\\_10](https://doi.org/10.1007/978-3-319-92507-3_10).

43. Zhang J, Hou Z, Wang X, Jiang H, Neng L, Zhang Y, et al. VEGFA165 gene therapy ameliorates blood-labyrinth barrier breakdown and hearing loss. *JCI Insight*. 2021;6:143285. <https://doi.org/10.1172/jci.insight.143285>.
44. Ishihara H, Kariya S, Okano M, Zhao P, Maeda Y, Nishizaki K. Expression of macrophage migration inhibitory factor and CD74 in the inner ear and middle ear in lipopolysaccharide-induced otitis media. *Acta Otolaryngol*. 2016;136:1011–6. <https://doi.org/10.1080/00016489.2016.1179786>.
45. Chai Y, He W, Yang W, Hetrick AP, Gonzalez JG, Sargsyan L, et al. Intratympanic Lipopolysaccharide elevates systemic fluorescent gentamicin uptake in the Cochlea. *Laryngoscope*. 2021;131:E2573–82. <https://doi.org/10.1002/lary.29610>.
46. Zou J, Poe D, Bjelke B, Pyykko I. Visualization of inner ear disorders with MRI in vivo: from animal models to human application. *Acta Otolaryngol Suppl*. 2009;22–31. <https://doi.org/10.1080/00016480902729850>.
47. Tanigawa T, Morikawa A, Hayashi K, Dan K, Tsuchihashi N, Goto F, et al. Auditory cells produce nitric oxide in response to bacterial lipopolysaccharide. *Innate Immun*. 2013;19:115–20. <https://doi.org/10.1177/1753425912450347>.
48. Watanabe K, Hess A, Bloch W, Michel O. Inhibition of inducible nitric oxide synthase lowers the cochlear damage by lipopolysaccharide in guinea pigs. *Free Radic Res*. 2000;32:363–70. <https://doi.org/10.1080/1071576000300361>.
49. Shi X, Dai C, Nuttall AL. Altered expression of inducible nitric oxide synthase (iNOS) in the cochlea. *Hear Res*. 2003;177:43–52. [https://doi.org/10.1016/S0378-5955\(02\)00796-7](https://doi.org/10.1016/S0378-5955(02)00796-7).
50. Imai K, Takeshita A, Hanazawa S. Transforming growth factor-beta inhibits lipopolysaccharide-stimulated expression of inflammatory cytokines in mouse macrophages through downregulation of activation protein 1 and CD14 receptor expression. *Infect Immun*. 2000;68:2418–23. <https://doi.org/10.1128/IAI.68.5.2418-2423.2000>.
51. Murillo-Cuesta S, Rodríguez-de la Rosa L, Contreras J, Celaya AM, Camarero G, Rivera T, et al. Transforming growth factor  $\beta$ 1 inhibition protects from noise-induced hearing loss. *Front Aging Neurosci*. 2015;7:32. <https://doi.org/10.3389/fnagi.2015.00032>.
52. Campbell DJ, Koch MA. Phenotypical and functional specialization of FOXP3 + regulatory T cells. *Nat Rev Immunol*. 2011;11:119–30. <https://doi.org/10.1038/nri2916>.
53. Rai V, Wood MB, Feng H, Schabla NM, Tu S, Zuo J. The immune response after noise damage in the cochlea is characterized by a heterogeneous mix of adaptive and innate immune cells. *Sci Rep*. 2020;10:15167. <https://doi.org/10.1038/s41598-020-72181-6>.
54. Zhou Y, Song F, Luo J. [The role of CD4 + CD25 + Treg in the mechanism of autoimmune auditory neuropathy in SD rats]. *Zhonghua Er Bi Yan Hou Tou Jing Wai Ke. Za Zhi*. 2023;58:225–32. <https://doi.org/10.3760/cma.j.cn115330-20220412-00183>.
55. Lee S-Y, Kim S, Han K, Woong Choi J, Byung Chae H, Yeon Choi D, et al. Microarray analysis of lipopolysaccharide-induced endotoxemia in the cochlea. *Gene*. 2022;823:146347. <https://doi.org/10.1016/j.gene.2022.146347>.
56. Xia L, Liu J, Sun Y, Shi H, Yang G, Feng Y, et al. Rosiglitazone improves glucocorticoid resistance in a Sudden Sensorineural hearing loss by promoting MAP kinase Phosphatase-1 expression. *Mediators Inflamm*. 2019;2019:7915730. <https://doi.org/10.1155/2019/7915730>.
57. Liu Z, Lu T, Liu S, Zhang F, Yang J, Dai S, et al. Long non-coding RNA NEAT1 contributes to lipopolysaccharide-induced inflammation and apoptosis of human middle ear epithelial cells via regulating the miR-301b-3p/TLR4 axis. *Exp Ther Med*. 2021;22:1360. <https://doi.org/10.3892/etm.2021.10795>.
58. Alexiou C, Arnold W, Fauser C, Schratzenstaller B, Gloddek B, Fuhrmann S, et al. Sudden sensorineural hearing loss: does application of glucocorticoids make sense? *Arch Otolaryngol Head Neck Surg*. 2001;127:253–8. <https://doi.org/10.1001/archotol.127.3.253>.
59. Meltser I, Canlon B. Protecting the auditory system with glucocorticoids. *Hear Res*. 2011;281:47–55. <https://doi.org/10.1016/j.heares.2011.06.003>.
60. Barrs DM. Intratympanic corticosteroids for Meniere's disease and vertigo. *Otolaryngol Clin North Am*. 2004;37:955–72. <https://doi.org/10.1016/j.otc.2004.03.004>.
61. Florea A, Zwart JE, Lee C-W, Depew A, Park SK, Inman J, et al. Effect of topical dexamethasone versus rimexolone on middle ear inflammation in experimental otitis media with effusion. *Acta Otolaryngol*. 2006;126:910–5. <https://doi.org/10.1080/00016480600606699>.
62. Pudrith C, Kim YH, Martin D, Gupta A, Inman J, Wareham R, et al. Effect of topical glucocorticoid treatment in chinchilla model of lipopolysaccharide induced otitis media with effusion. *Int J Pediatr Otorhinolaryngol*. 2010;74:1273–5. <https://doi.org/10.1016/j.ijporl.2010.08.003>.
63. Madamsetty VS, Mohammadinejad R, Uzieliene I, Nabavi N, Dehshahri A, Garcia-Couce J, et al. Dexamethasone: insights into pharmacological aspects, therapeutic mechanisms, and Delivery Systems. *ACS Biomater Sci Eng*. 2022;8:1763–90. <https://doi.org/10.1021/acsbomaterials.2c00026>.
64. Park K, Jin J, Hu Y, Zhou K, Ma J. Overexpression of pigment epithelium-derived factor inhibits retinal inflammation and neovascularization. *Am J Pathol*. 2011;178:688–98. <https://doi.org/10.1016/j.ajpath.2010.10.014>.
65. Zhang D-G, Yu W-Q, Liu J-H, Kong L-G, Zhang N, Song Y-D, et al. Serum/glucocorticoid-inducible kinase 1 deficiency induces NLRP3 inflammasome activation and autoinflammation of macrophages in a murine endolymphatic hydrops model. *Nat Commun*. 2023;14:1249. <https://doi.org/10.1038/s41467-023-36949-4>.
66. Nakanishi H, Yamada S, Kita J, Shinmura D, Hosokawa K, Sahara S et al. Auditory and vestibular characteristics of NLRP3 Inflammasome Related Autoinflammatory Disorders: monogenic hearing loss can be improved by anti-interleukin-1 therapy. *Frontiers in Neurology* 2022;13.

## Publisher's Note

Springer Nature remains neutral with regard to jurisdictional claims in published maps and institutional affiliations.